Supporting Information

De-coupling Fluorous Protein Coatings Yield Heat Stable and Intrinsically Sterile Bioformulations

Harminder Singh[1], Atip Lawanprasert[1], Utkarsh[1], Sopida Pimcharoen[1], Arshiya Dewan[2], Dane Rahoi[3], Girish S. Kirimanjeswara[2,4,5], and Scott H. Medina*[,1,6]

[1]*Department of Biomedical Engineering, Pennsylvania State University, University Park, PA, USA, 16802-4400*

[2]*Department of Veterinary and Biomedical Sciences, Pennsylvania State University, University Park, PA, USA, 16802-4400*

[3]*Animal Diagnostics Laboratory, Pennsylvania State University, University Park, PA, USA, 16802-4400*

[4]*Center for Infectious Disease Dynamics, Pennsylvania State University, University Park, PA, USA, 16802-4400*

[5]*Center for Molecular Immunology and Infectious Disease, Pennsylvania State University, University Park, PA, USA, 16802-4400*

[6]*Huck Institutes of the Life Sciences, Pennsylvania State University, University Park, PA, USA, 16802-4400*

*corresponding email: shm126@psu.edu

Content **Page Number**

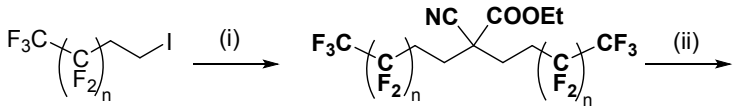

1a; n = 5
1b; n = 7
1c; n = 3

2a; n = 5
2b; n = 7
2c; n = 3

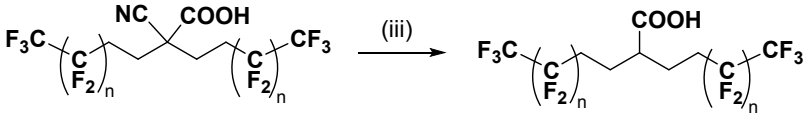

PD-6; n = 5
PD-8; n = 7
PD-10; n = 3

PD-7; n = 5
PD-9; n = 7
PD-11; n = 3

Scheme S1: Synthetic diagram for protein dispersants PD-6 to PD-11; Reagents and conditions: (i) Ethyl cyanoacetate, K_2CO_3, DMF, RT, N_2; (b) aq. KOH, C_2H_5OH:H_2O = 1:1; 80^oC (iii) (a) Conc. HCl, 100^oC, 2h; (b) Conc. H_2SO_4, 150^oC, 24h.

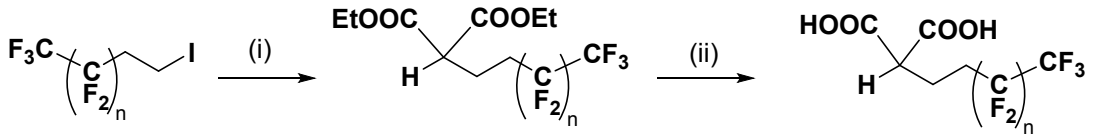

1a; n = 5
1b; n = 7
1c; n = 3

3a; n = 5
3b; n = 7
3c; n = 3

PD-12; n = 5
PD-13; n = 7
PD-14; n = 3

Scheme S2: Synthetic diagram for protein dispersants PD-12 to PD-14; Reagents and conditions: (i) Diethyl malonate, K_2CO_3, DMF, RT, N_2; (b) aq. KOH, C_2H_5OH:H_2O = 1:1; 80^oC.

Synthetic methods for intermediates 2a-2c and 3a-3c

General procedure for the synthesis of intermediates 2a-2c: To a 100 mL round bottom flask, kept under a nitrogen atmosphere, containing flame dried K_2CO_3 (538 mg, 2.2 equiv, 3.89 mmol) and ethyl cyanoacetate (200 mg, 1.0 equiv., 1.77 mmol) dissolved in anhydrous DMF (5 mL), perfluoroalkyl ethyl iodide 1a/1b/1c (2.1 equiv., 3.71 mmol) was added. This reaction mixture was stirred at room temperature and the progress of the reaction was monitored using thin-layer chromatography (TLC). The TLC showed the completion of the reaction in 24 h. Cold water was added to the reaction mixture and extracted using ethyl acetate. The ethyl acetate layer was concentrated in vacuo to give crude product that was purified using Flash chromatography having silica as stationary phase and ethyl acetate:hexanes mixture as mobile phase to give pure cyanoacetate derivates 2a-2c as colorless solid (Scheme S1).

2a: Yield = 1.10 g (77%); ^{1}H NMR (400 MHz, $CDCl_3$) δ 4.37 (q, *J* = 7.1 Hz, 2H), 2.50 – 2.08 (m, 8H), 1.36 (t, *J* = 7.1 Hz, 3H) ppm; ^{19}F NMR (376 MHz, $CDCl_3$) δ -80.78 (t, *J* = 9.9 Hz, 6F), -114.17 – -114.34 (m, 4F), -121.81 – -121.98 (m, 4F), -122.74 – -122.98 (m, 4F),-123.10 – -123.26 (m, 4F), -126.14 (m, 4H) ppm; ^{13}C NMR (100 MHz, $CDCl_3$) δ 167.05, 120.09-108.06 (m, CF_n peaks), 117.12, 64.18, 47.80, 28.21 (t, J_{CF} = 4.4 Hz), 27.42 (t, J_{CF} = 22.4 Hz), 14.17 ppm.

2b: Yield = 1.25 g (70%); ^{1}H NMR (400 MHz, $CDCl_3$) δ 4.37 (d, *J* = 7.1 Hz, 2H), 2.47 – 2.08 (m, 8H), 1.36 (t, *J* = 7.1 Hz, 3H) ppm; ^{19}F NMR (376 MHz, $CDCl_3$) δ -80.74 (t, *J* = 10.1 Hz, 6F), -114.22 (t, *J* = 14.3 Hz, 4F), -121.60 – -121.80 (m, 4F), 122.00 – -121.80 (m, 8F) -122.60 – 122.80 (m, 4F), -123.05 – -123.20 (m, 4H), -126.03 – -126.19 (m, 4H) ppm; ^{13}C NMR (100 MHz, $CDCl_3$) δ 166.84, 116.92, 63.98, 47.58, 28.19, 27.42 (t, J_{CF} = 22.5 Hz), 13.98 ppm.

2c: Yield = 0.80 g (75%); ^{1}H NMR (400 MHz, $CDCl_3$) δ 4.37 (q, *J* = 7.1 Hz, 2H), 2.49 – 2.08 (m, 8H), 1.36 (t, *J* = 7.1 Hz, 3H) ppm; ^{19}F NMR (376 MHz, $CDCl_3$) δ -81.10 (tt, *J* = 9.7, 3.2 Hz, 6F), -114.56 (t, *J* = 13.7 Hz, 4F), -124.14 – -124.25 (m, 4F), -126.11 (dt, *J* = 13.2, 6.6 Hz, 4F) ppm; ^{13}C NMR (100 MHz, $CDCl_3$) δ 167.05, 120.04 – 107.90 (m, CF_n peaks), 117.11, 64.17, 47.81, 28.38 (t, J_{CF} = 4.5 Hz), 27.52 (t, J_{CF} = 22.4 Hz), 14.15 ppm.

General procedure for the synthesis of intermediates 3a-3c: Anhydrous DMF (8 mL) was transferred to a 100 mL round bottomed flask containing NaH (60% suspension in mineral oil that was washed with hexanes prior to use) (125 mg, 3.12 mmol, 2.5 equiv.) that maintained an inert atmosphere with constant N_2 purging. To this mixture, diethylmalonate (200 mg, 1.25 mmol, 1.0 equiv.) was added and stirred for 1 h at room temperature. A solution of perfluoroalkyl ethyl iodide 1c/1b/1c (1.1 equiv., 1.37 mmol) in THF (2 mL) was added to the reaction mixture and stirred with heating at 80^{o}C for 12h. After completion, the reaction was quenched with saturated ammonium chloride solution followed by extraction with ethyl acetate. The ethyl acetate layer obtained upon washing with brine solution and drying with Na_2SO_4 was concentrated in vacuo to get crude product as a brown oil. Flash chromatography of crude product using ethyl acetate: hexanes mixture as eluent gave colorless liquid as final product (Scheme S2).

3a: Yield = 380 mg (60%); ^{1}H NMR (400 MHz, $CDCl_3$) δ 4.23 (qd, *J* = 7.2, 2.8 Hz, 4H), 3.46 – 3.38 (m, 1H), 2.30 – 2.09 (m, 4H), 1.28 (t, *J* = 7.1 Hz, 6H) ppm; ^{19}F NMR (376 MHz, $CDCl_3$) δ -80.80 (t, *J* = 10.1 Hz, 3F), -114.55 (m, 2F), -121.81 – -122.07 (m, 2F), -122.78 – -123.05 (m, 2F), -123.480 – -123.56 (m, 2F), -126.08 – -126.26 (m, 2F) ppm; ^{13}C NMR (100 MHz, $CDCl_3$) δ 168.49, 61.82, 50.70, 28.48 (t, J_{CF} = 22.0 Hz), 19.72, 14.03 ppm.

3b: Yield = 350 mg (46%); ^{1}H NMR (400 MHz, $CDCl_3$) δ 4.25 (qd, *J* = 7.1, 2.7 Hz, 4H), 3.47 – 3.40 (m, 1H), 2.29 – 2.14 (m, 4H), 1.30 (t, *J* = 7.1 Hz, 6H) ppm; ^{19}F NMR (376 MHz, $CDCl_3$) δ -81.04

(tt, *J* = 9.3, 3.3 Hz, 3F), -114.77 (m, 2F), -124.42 (m, 2F), -126.05 (m, 2F) ppm; ^{13}C NMR (100 MHz, $CDCl_3$) δ 168.47, 61.80, 50.68, 28.38 (t, J_{CF} = 22.0 Hz), 19.68, 14.03 ppm.

3c: Yield = 250 mg (49%); ^{1}H NMR (400 MHz, $CDCl_3$) δ 4.23 (qd, *J* = 7.1, 2.9 Hz, 4H), 3.47 – 3.37 (m, 1H), 2.20 (d, *J* = 4.0 Hz, 4H), 1.28 (t, *J* = 7.1 Hz, 6H) ppm; ^{19}F NMR (376 MHz, $CDCl_3$) δ -80.78 (t, *J* = 10.0 Hz, 3F), -114.34 – -114.67 (m, 2F), -121.62 – -121.79 (m, 2F), -121.84 – -122.04 (m, 4F), -122.63 – -122.85 (m, 2F), -123.24 – -123.61 (m, 2F), -126.06 – -126.20 (m, 2F) ppm; ^{13}C NMR (100 MHz, CDC I_3) δ 168.50, 61.82, 50.71, 28.50 (t, J_{CF} = 22.1 Hz), 19.30 (t, J_{CF} = 4.5 Hz), 14.03 ppm.

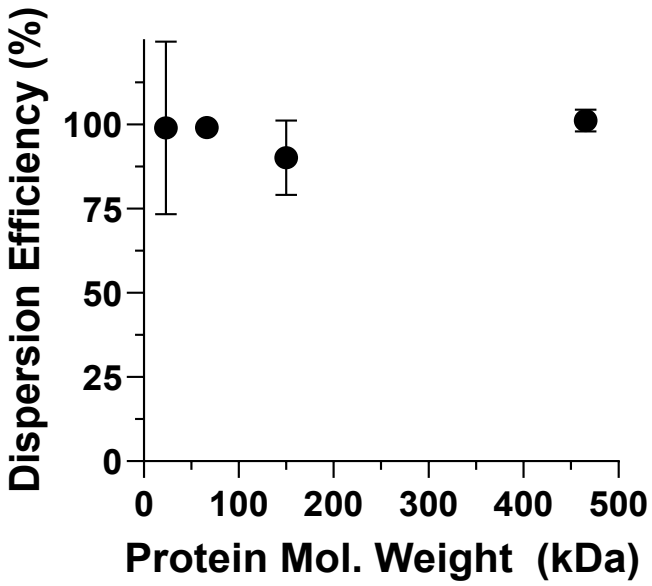

Figure S1: Relationship of PD-7 dispersion efficiency to protein molecular weight.

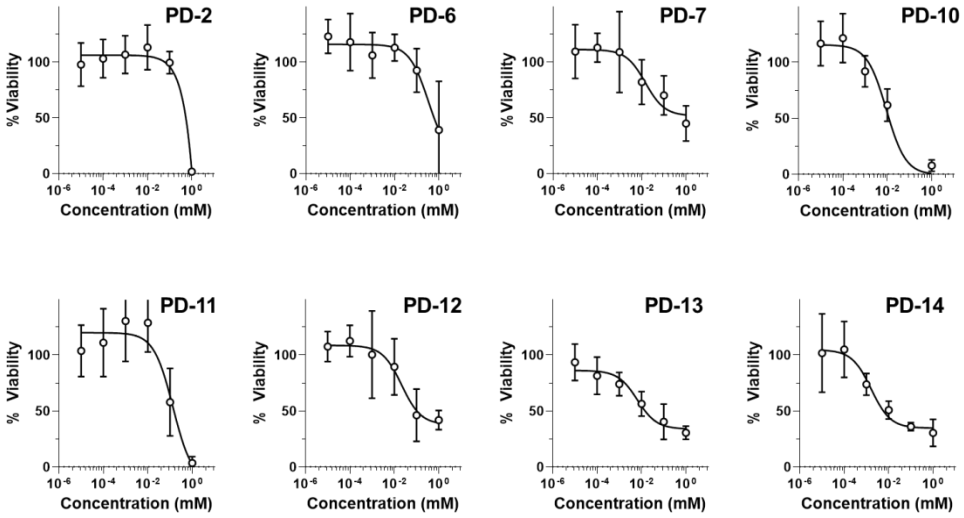

Compound	IC_{50} (mM)
PD-2	0.54
PD-6	0.61
PD-7	~ 1.00
PD-10	0.01
PD-11	0.15
PD-12	0.10
PD-13	0.01
PD-14	0.01

Figure S2: Cytotoxicity curves for the indicated protein dispersant towards HepG2 human hepatic carcinoma cells. The concentration at which 50% inhibition of cell (IC_{50}) occurs is tabulated on the right.

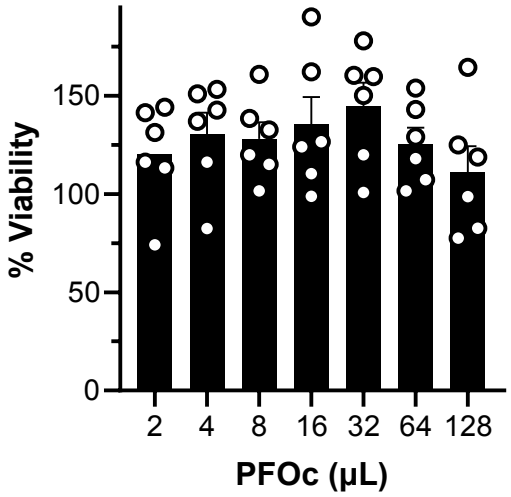

Figure S3: Percent viability of HepG2 cells cultured in increasing volumes of PFOc added to the cell culture media.

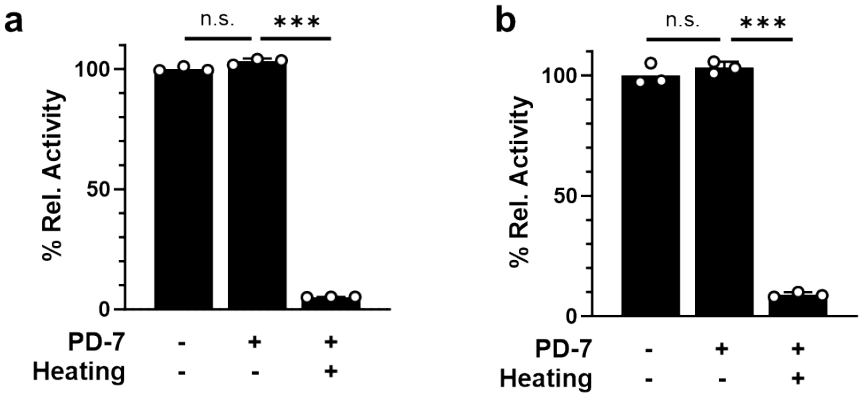

Figure S4: Bioactivity of (**a**) β-gal and (**b**) trypsin in PBS without/with 1mM PD-7 before (-, 25°C) and after (+) heating at 90°C for 30 minutes. Statistical significance between conditions is indicated by a line, using unpaired Student's t-test with n.s. = not significant and *** $p<0.001$.

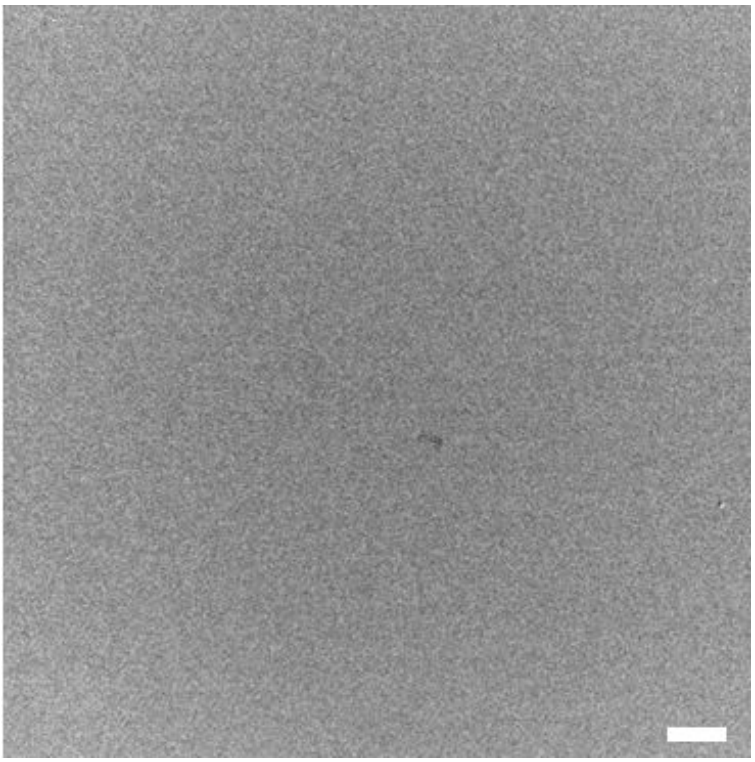

Figure S5: Representative transmission electron micrograph of monomeric BSA proteins in water. Scale bar represents 100 μm.

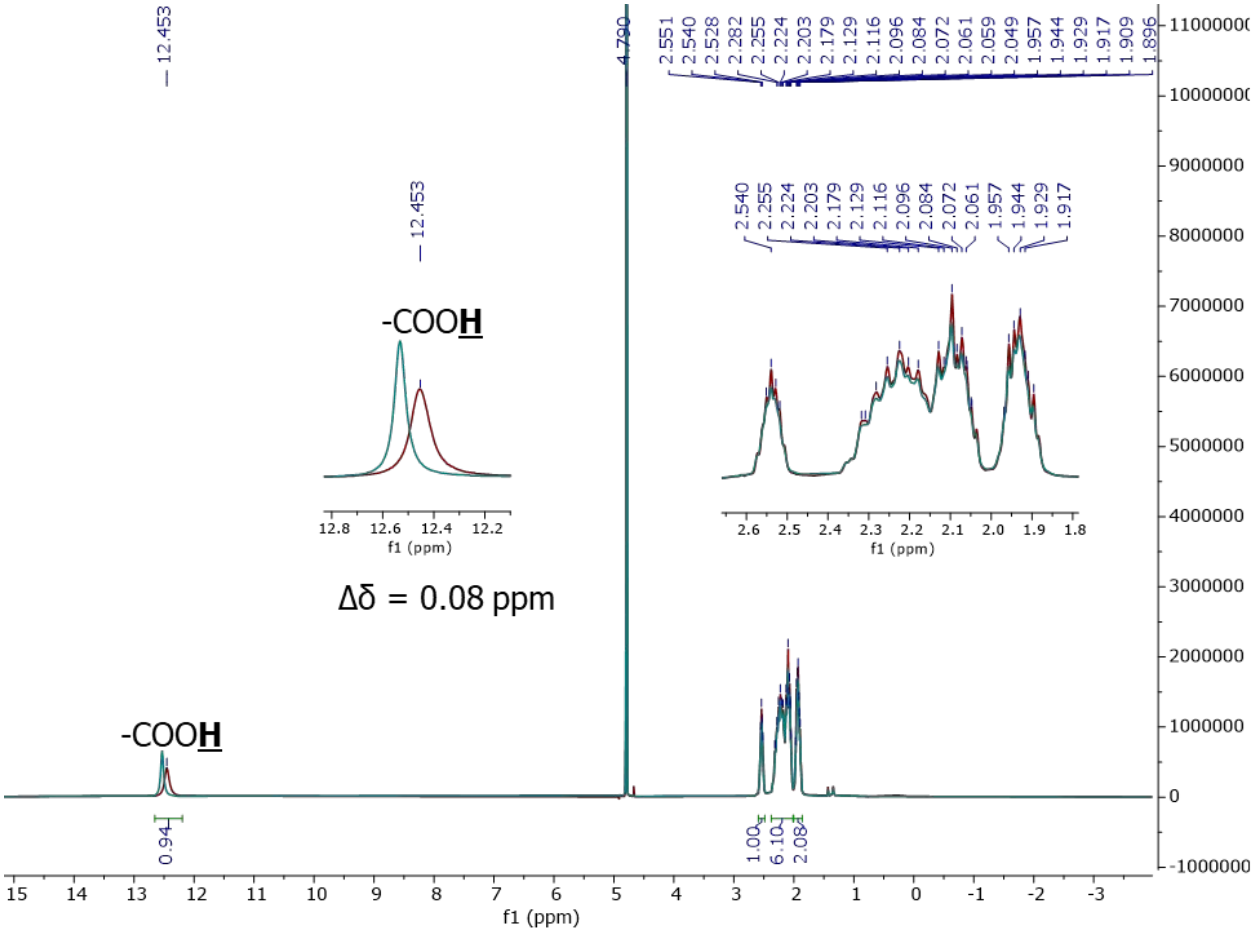

Figure S6: Superimposed ^{1}H NMR spectra of PD-7 (60 mM, maroon) and PD-7:BSA complex (1000:1 molar ratio, teal). Inset shows magnified region of PD-7's -COO**H** proton chemical shift (Δδ).

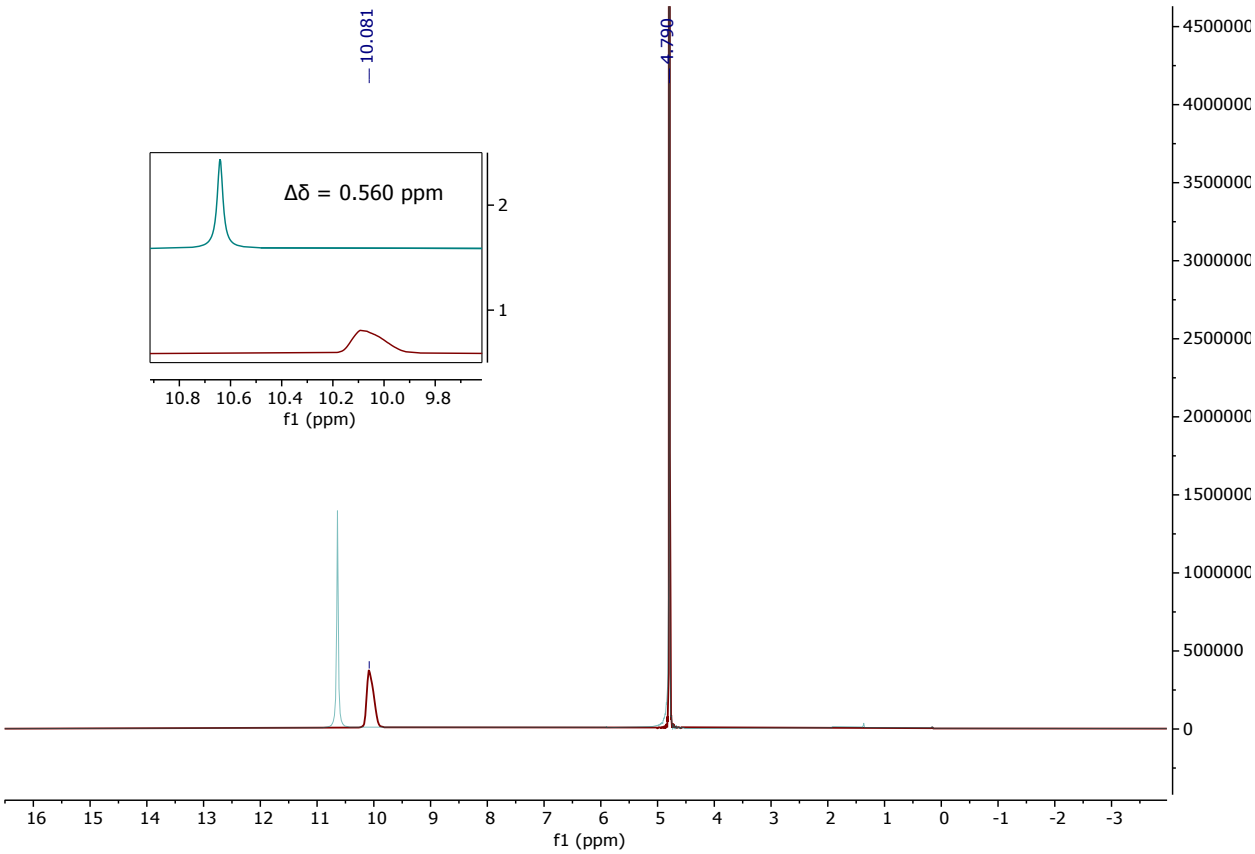

Figure S7: Superimposed ^{1}H NMR spectra of PD-2 (60 mM, maroon) and PD-2:BSA complex (1000:1 molar ratio, teal). Inset shows magnified region of PD-2's -COO**H** proton chemical shift (Δδ).

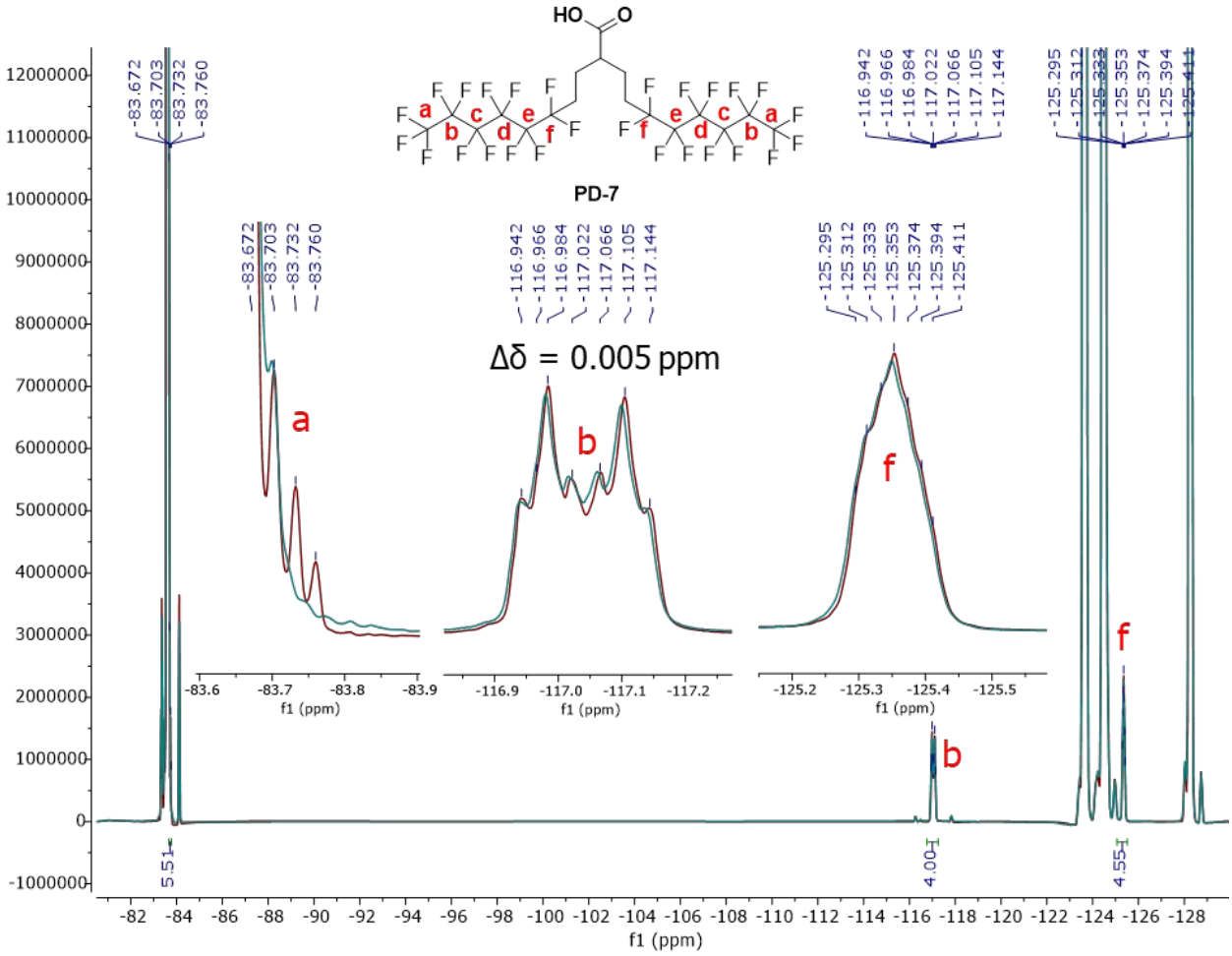

Figure S8: Superimposed ^{19}F NMR spectra of PD-7 (60 mM, maroon) and PD-7:BSA complex (1000:1 molar ratio, teal). Inset shows magnified region of PD-7's -C**F**$_x$ chemical shift (Δδ).

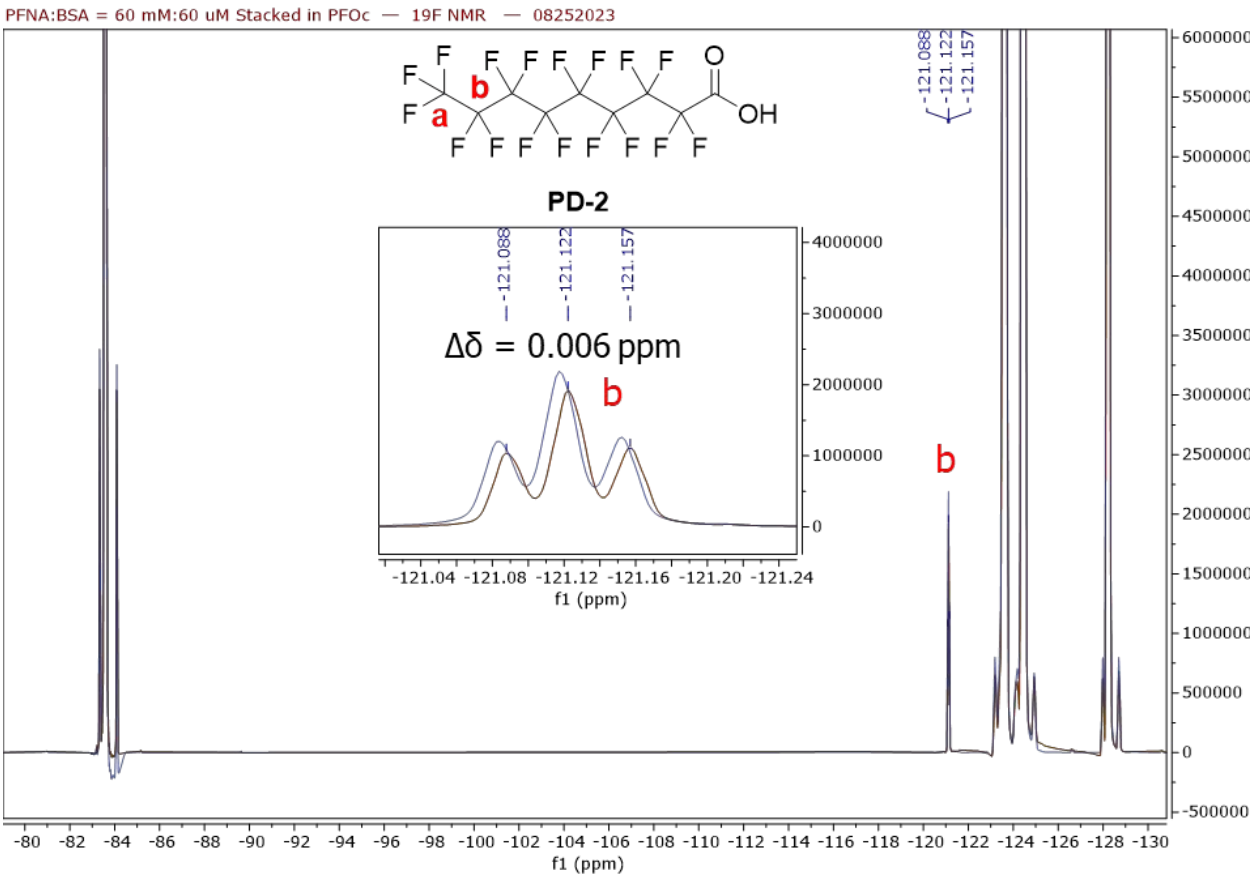

Figure S9: Superimposed ^{19}F NMR spectra of PD-2 (60 mM, maroon) and PD-2:BSA complex (1000:1 molar ratio, teal). Inset shows magnified region of PD-2's -C**F**$_x$ chemical shift (Δδ).

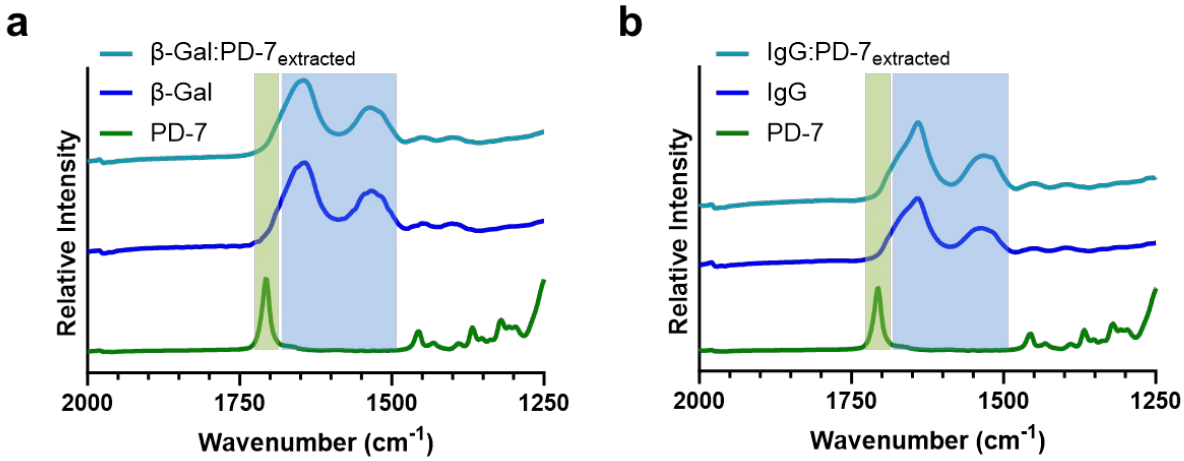

Figure S10: Stacked FTIR spectra of (a) β-Gal and (b) IgG proteins (blue), PD-7 (green), and the PD-7:protein complex after extraction into PBS (teal). Green and blue shading highlight PD-7 and protein specific spectral features, respectively.

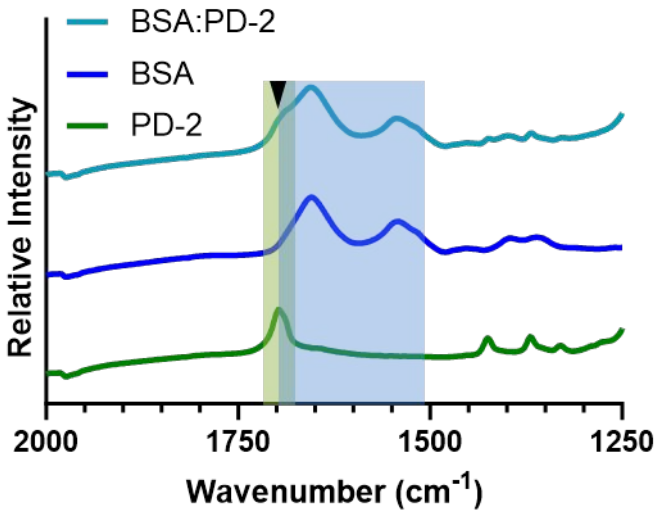

Figure S11: Stacked FTIR spectra of PD-2 (green), BSA (blue) and the PD-2:BSA complex after elution into PBS (turquoise). Green and blue shading represent PD-2 and BSA spectral features, respectively. Arrow delineates presence of PD-2 spectral signal in PD-2:BSA sample.

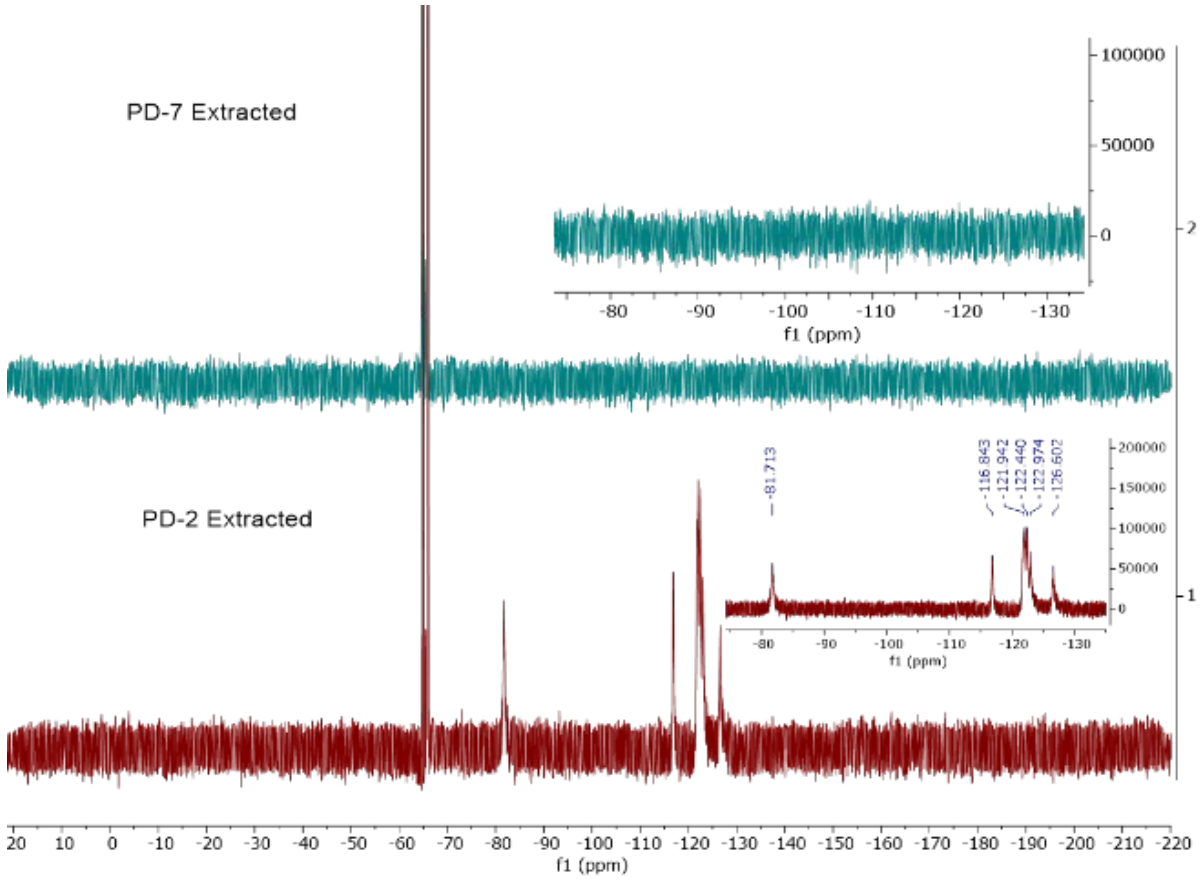

Figure S12: ^{19}F NMR spectra of PD-7 (teal, 30mM) and PD-2 (maroon, 30mM) after complexation with BSA (1000:1 molar ratio) and elution into PBS. Inset shows characteristic spectral regions of each dispersant. Lack of signal in the PD-7 extracted sample suggests this dispersant de-couples from the protein biologic in physiologic solutions and remains in the PFOc phase.

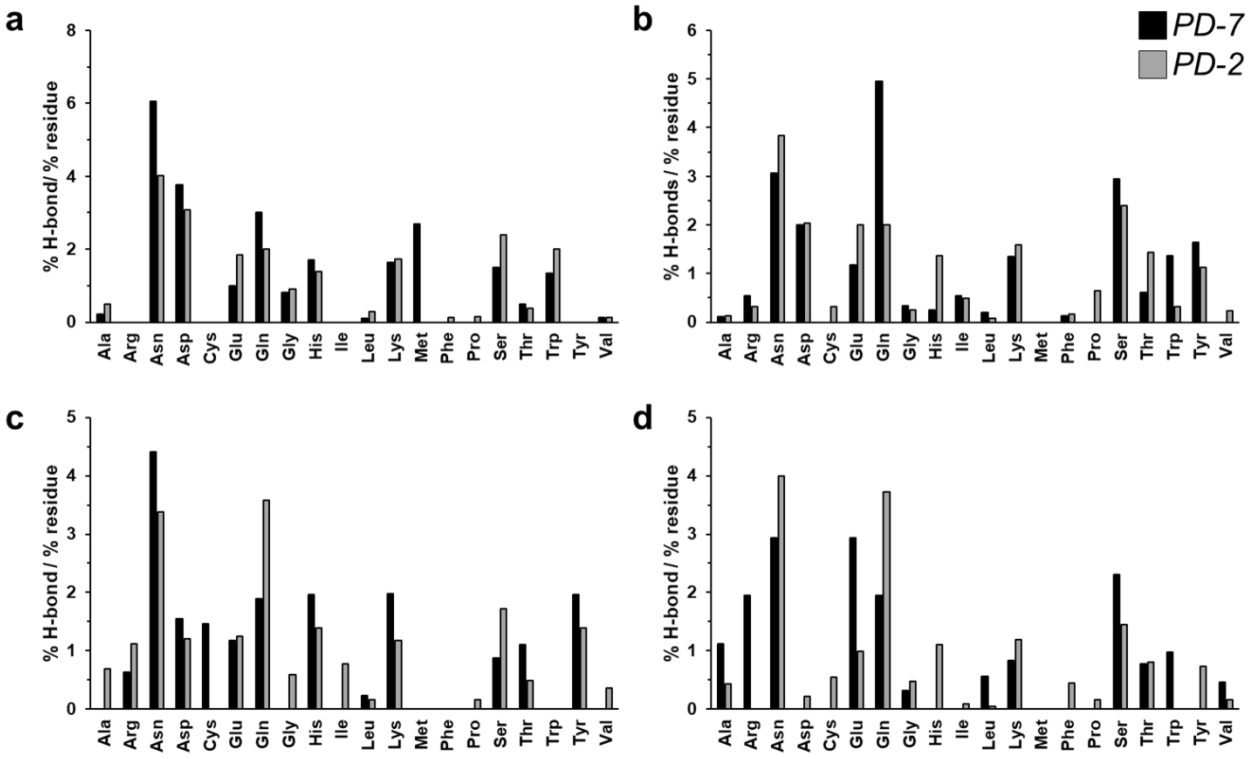

Figure S13: Residue-specific hydrogen-bonding interactions of PD-7 (black) or PD-2 (grey) with (**a**) Hb, (**b**) β-Gal, (**c**) GFP and (**d**) trypsin. Data reported as the percentage of total hydrogen bonds divided by the frequency normalized residue count in the protein.

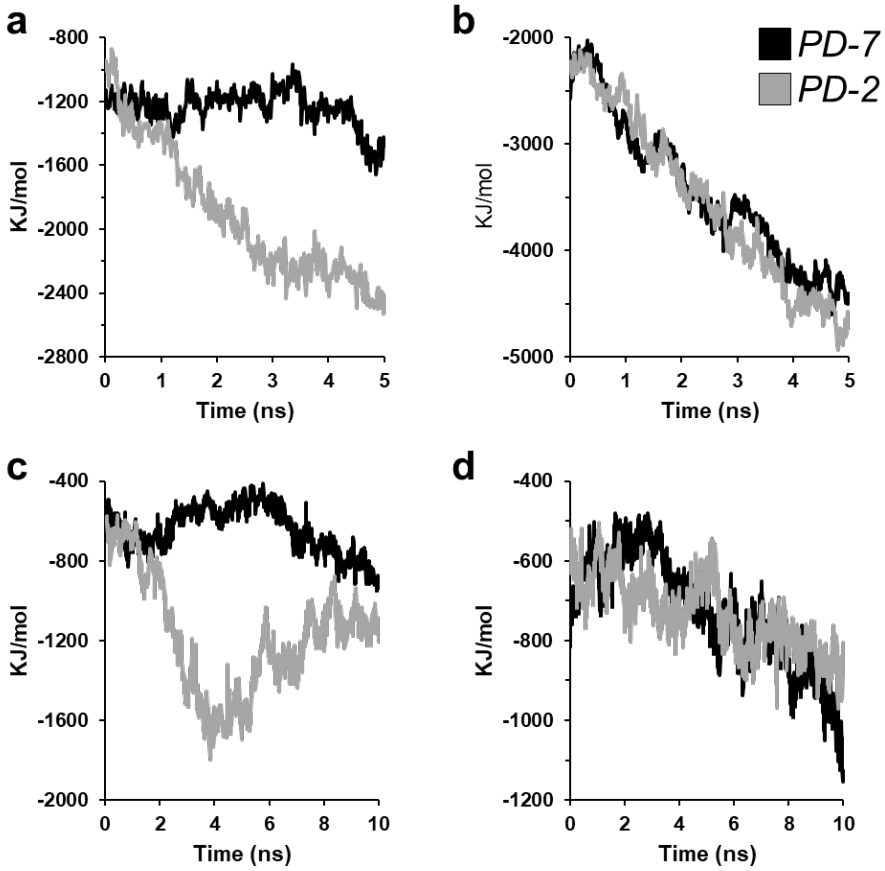

Figure S14: Change in interaction energy of PD-7 (black) or PD-2 (grey) after ligand binding to the surface of (**a**) Hb, (**b**) β-Gal, (**c**) GFP or (**d**) trypsin proteins.

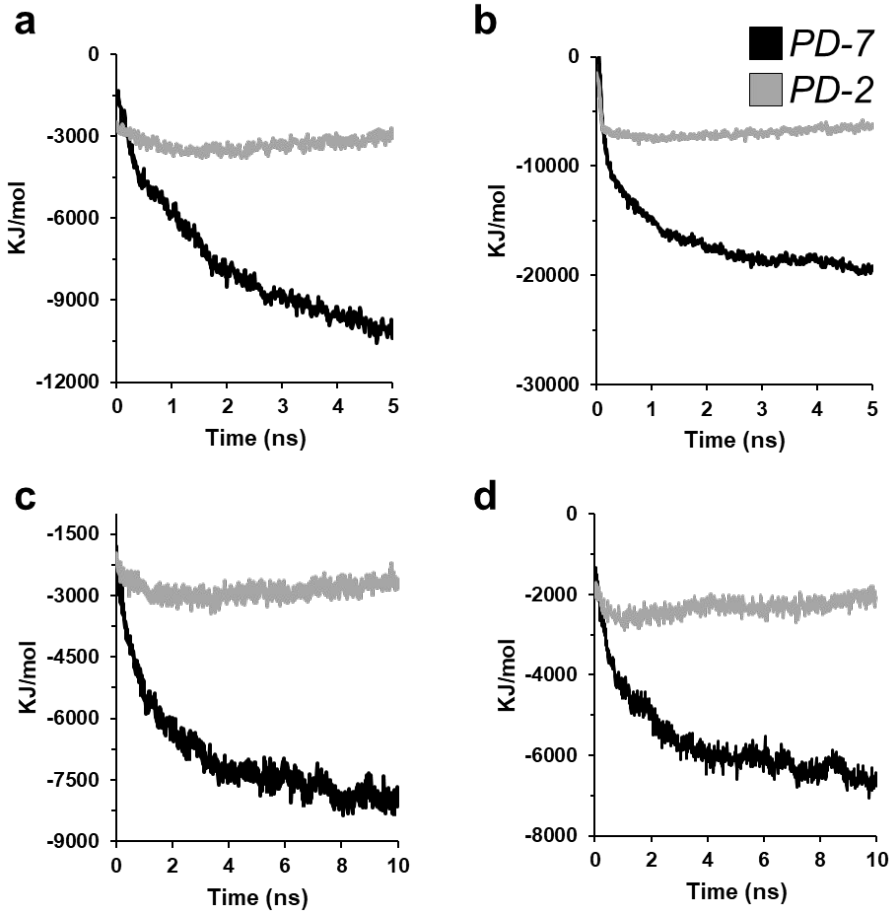

Figure S15: Change in interaction energy of PD-7 (black) or PD-2 (grey) during dispersant oligomerization in the presence of (**a**) Hb, (**b**) β-Gal, (**c**) GFP or (**d**) trypsin proteins.

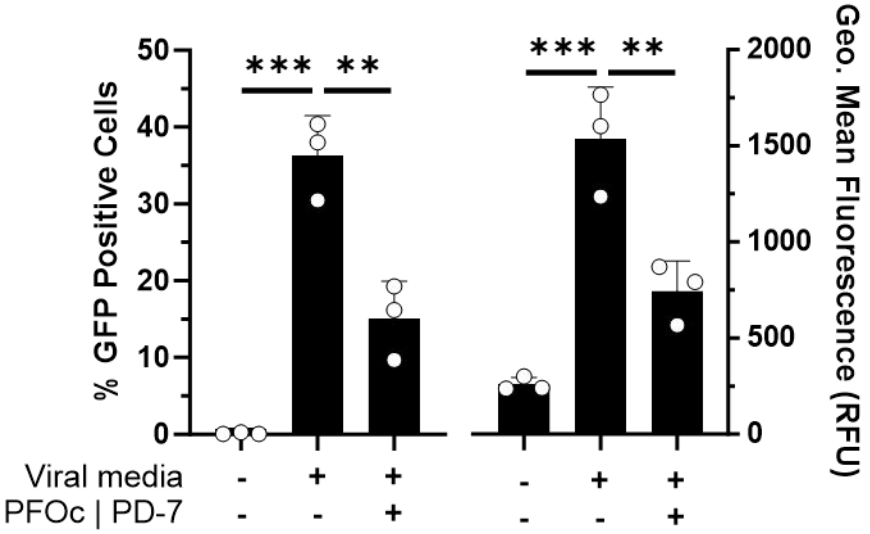

Figure S16: (*Left)* Percent GFP positive and (*Right*) geometric mean fluorescence of HEK293 cells after incubation in the absence (-) or presence (+) of GFP-lentiviral transfection vectors formulated in cell culture media (viral media), or pre-dispersed in PFOc and PD-7 formulations (PFOc | PD-7) before extraction into the treatment cell culture media. Statistical significance between conditions is indicated by a line, using unpaired Student's t-test with ** $p<0.01$ and *** $p<0.001$.

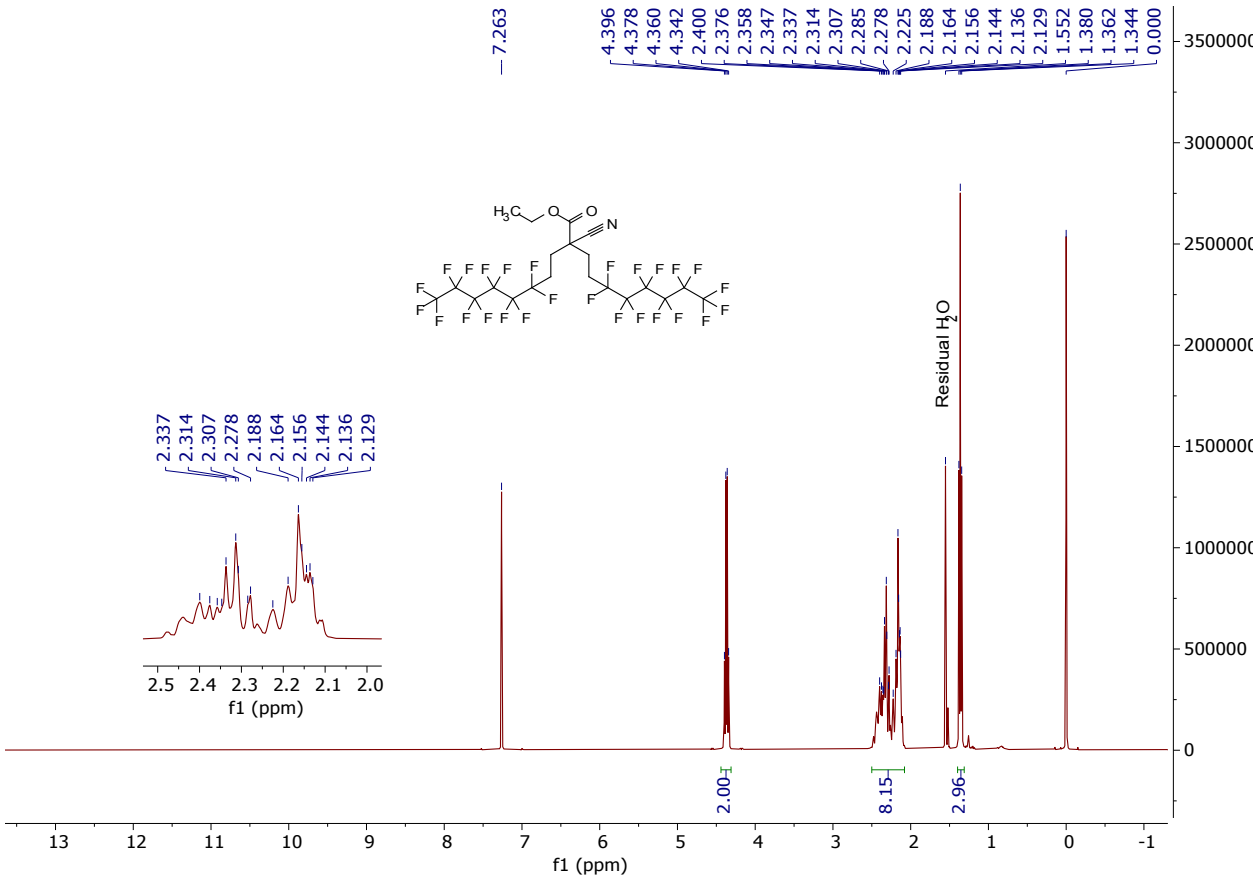

Figure S17. ^{1}H NMR spectrum of compound 2a.

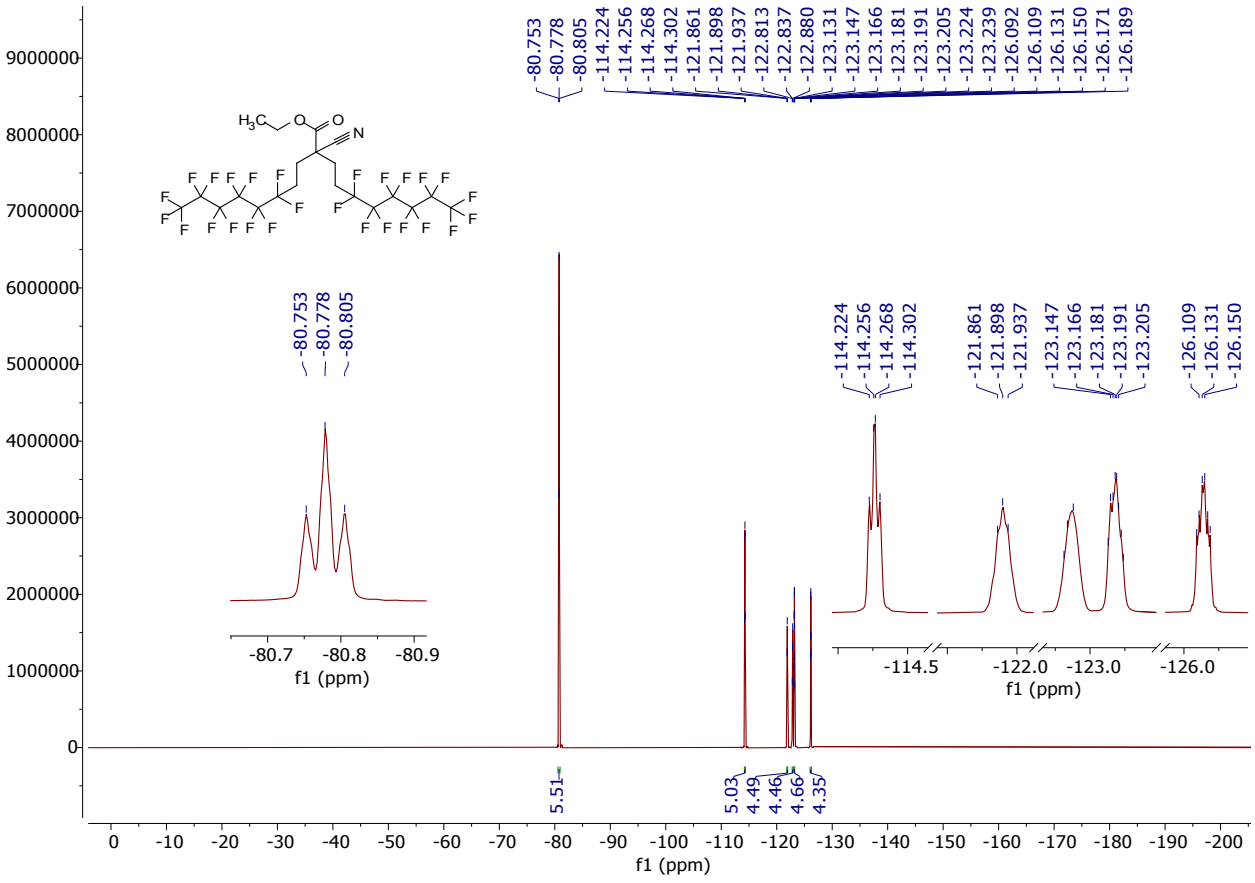

Figure S18. ^{19}F NMR spectrum of compound 2a.

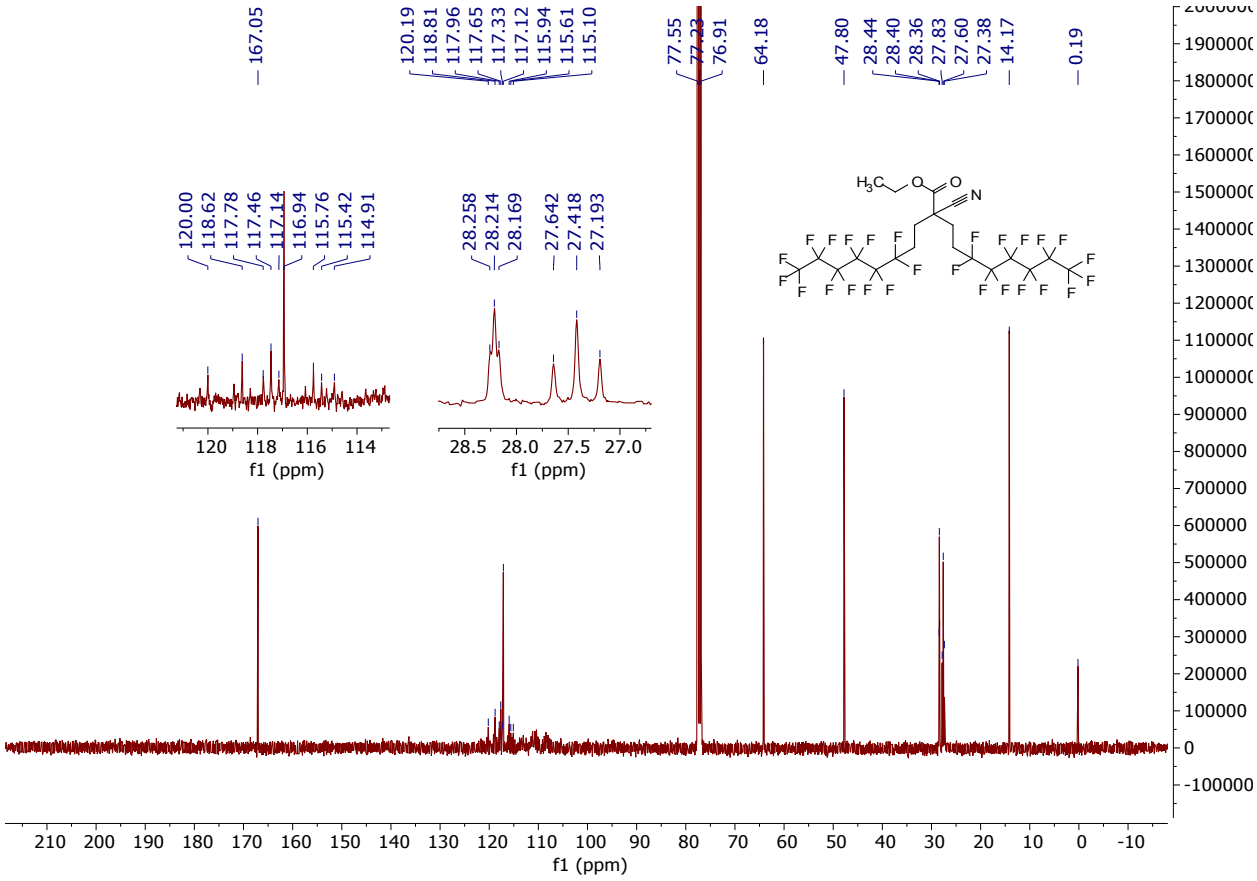

Figure S19. ^{13}C NMR spectrum of compound 2a.

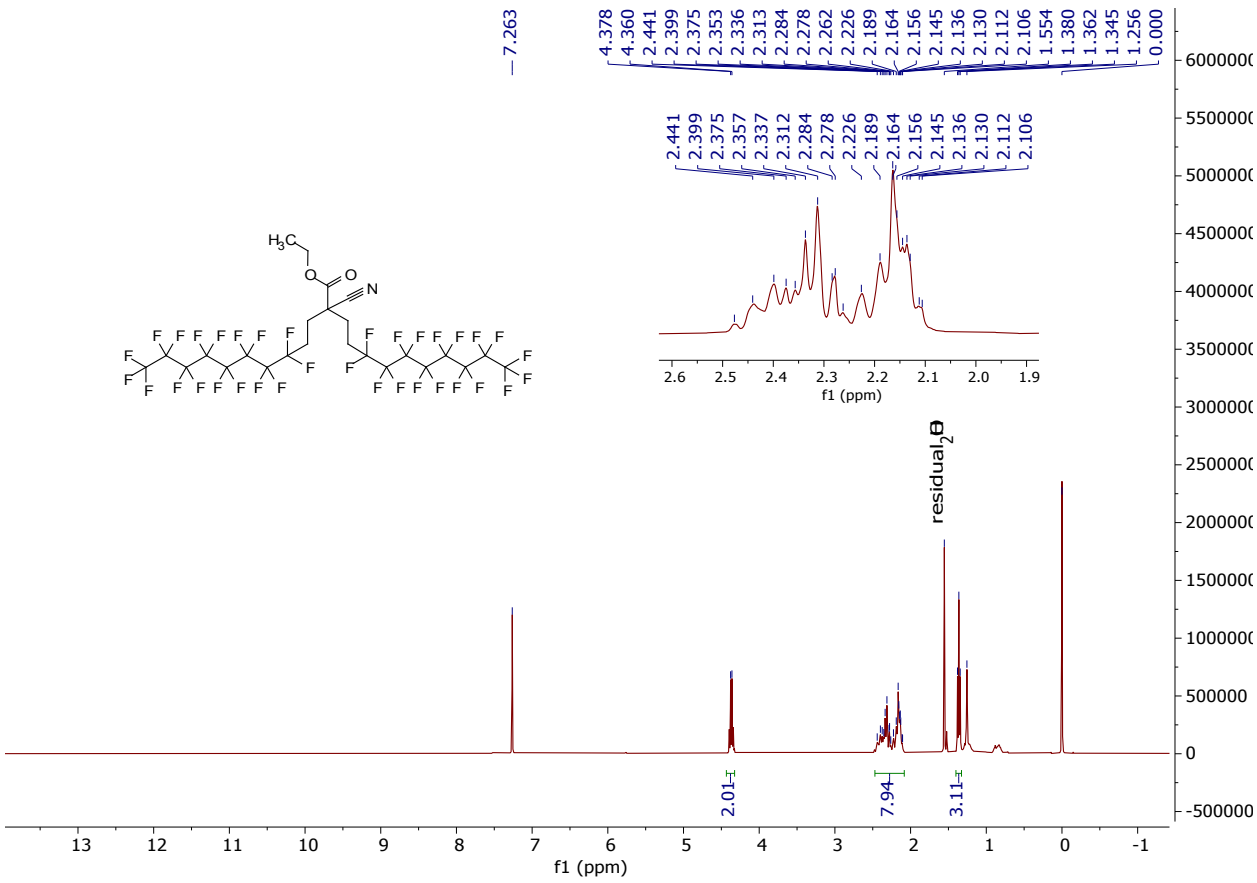

Figure S20. ^{1}H NMR spectrum of compound 2b.

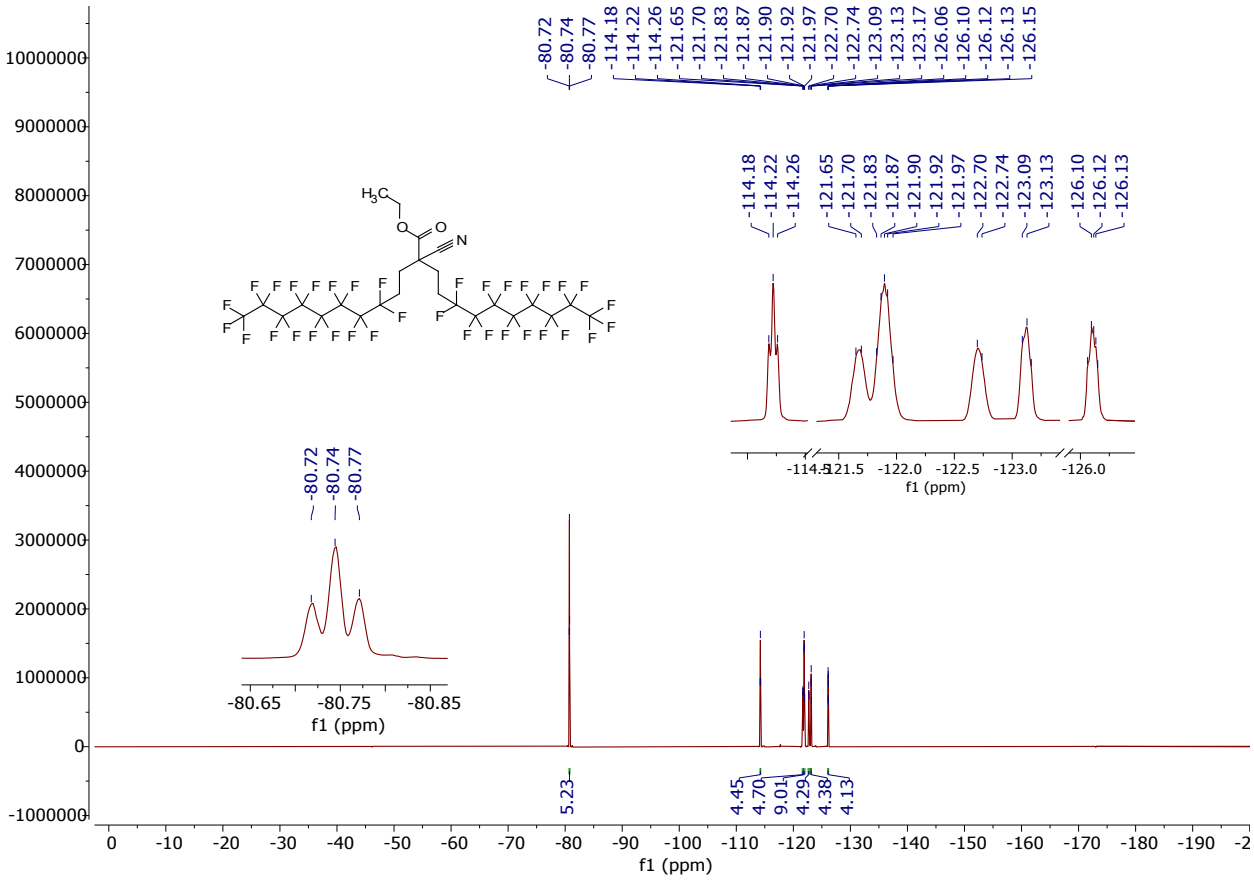

Figure S21. ^{19}F NMR spectrum of compound 2b.

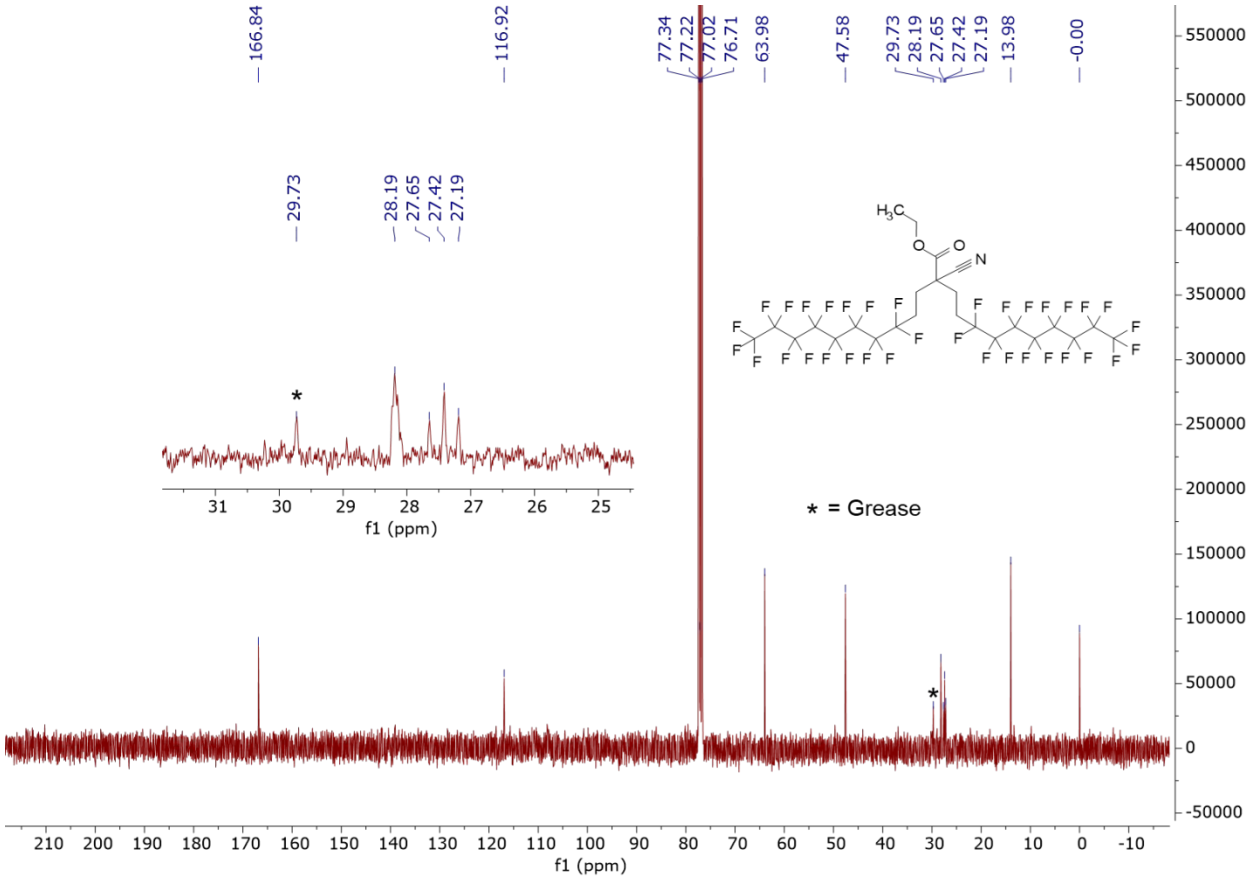

Figure S22. ^{13}C NMR spectrum of compound 2b.

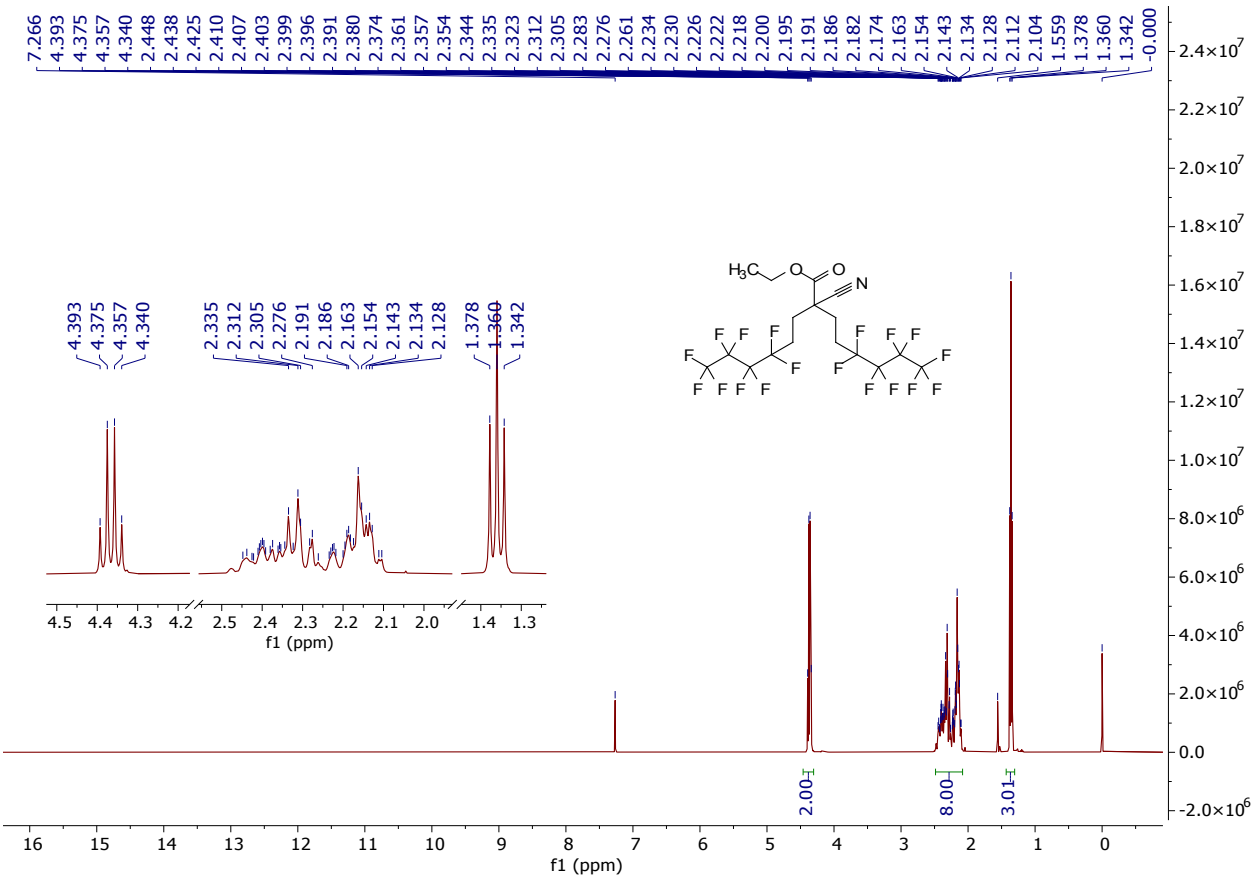

Figure S23. ^{1}H NMR spectrum of compound 2c.

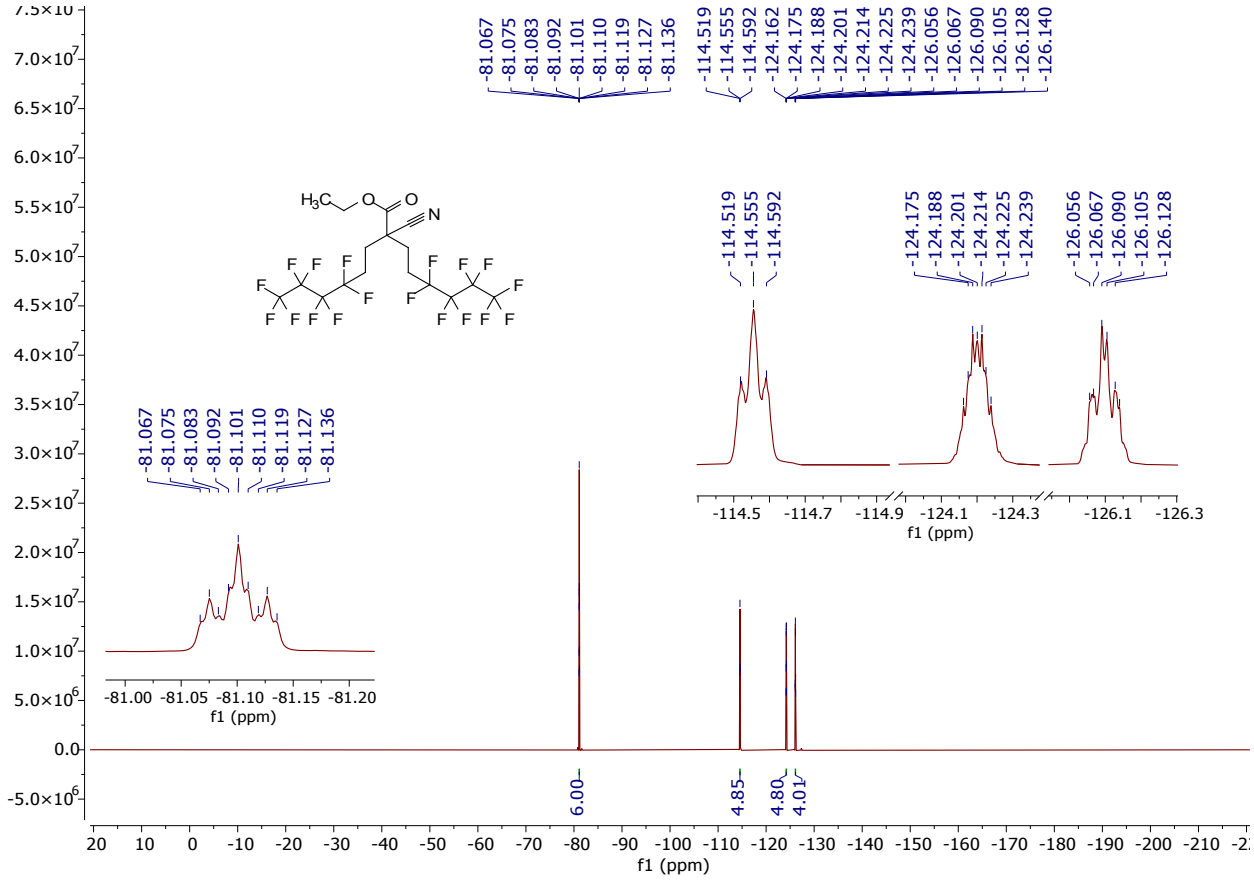

Figure S24. ^{19}F NMR spectrum of compound 2c.

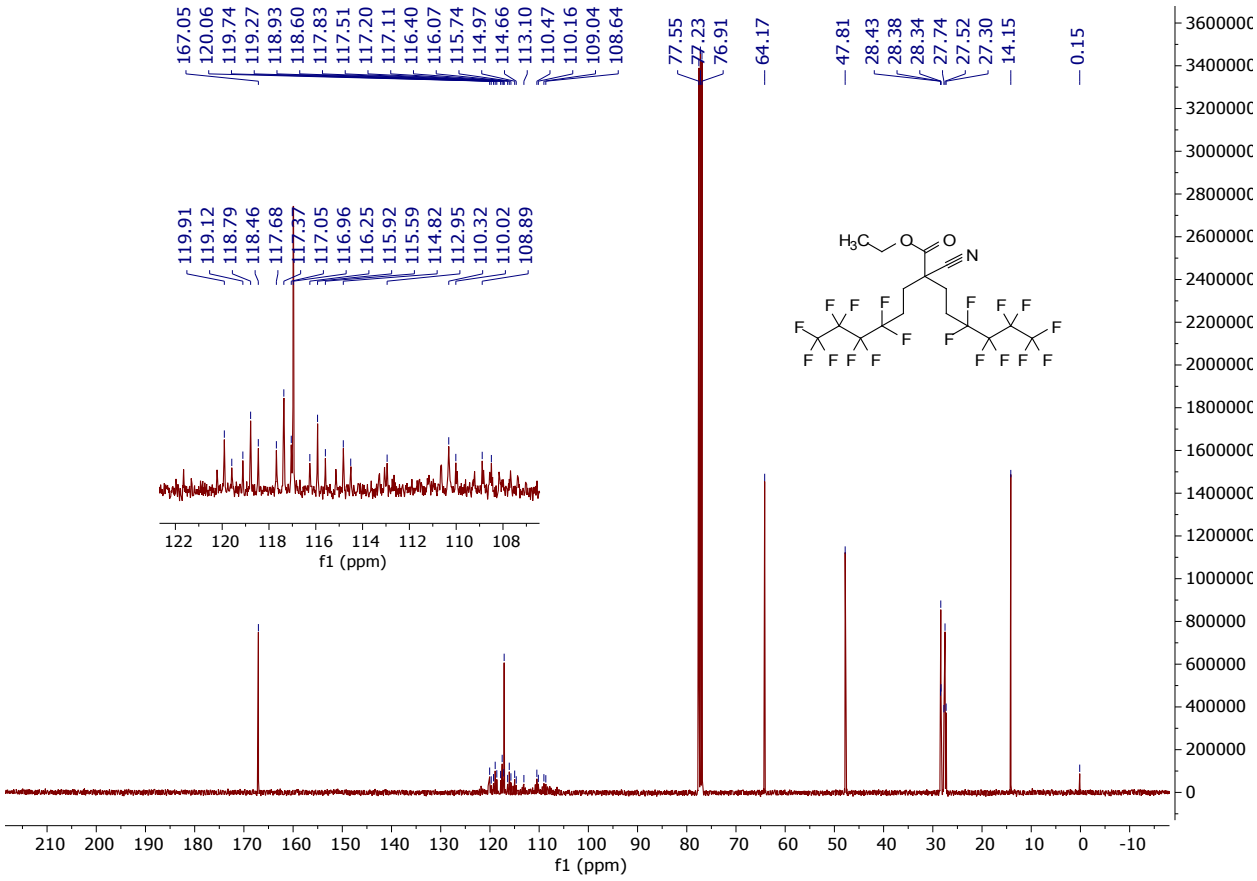

Figure S25. ^{13}C NMR spectrum of compound 2c.

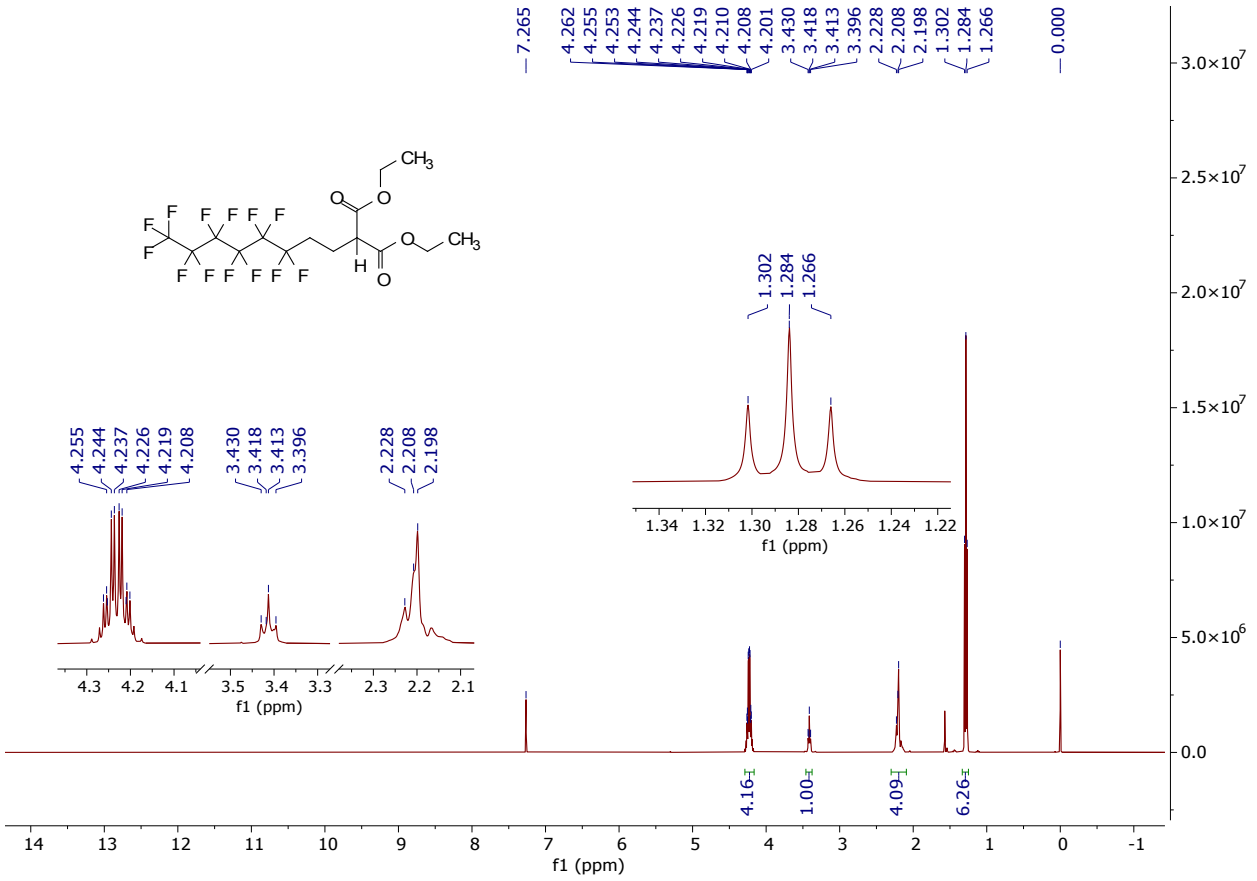

Figure S26. ^{1}H NMR spectrum of compound 3a.

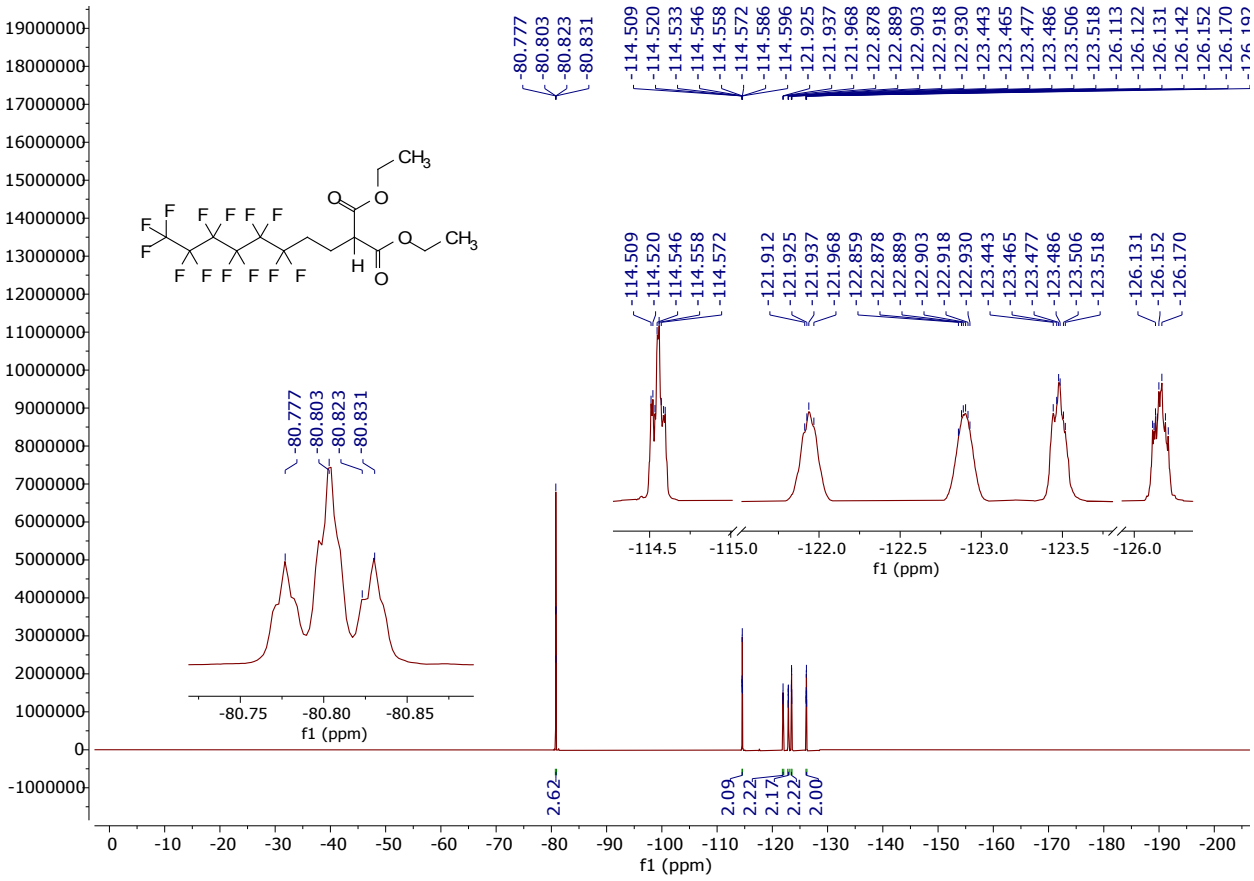

Figure S27. ^{19}F NMR spectrum of compound 3a.

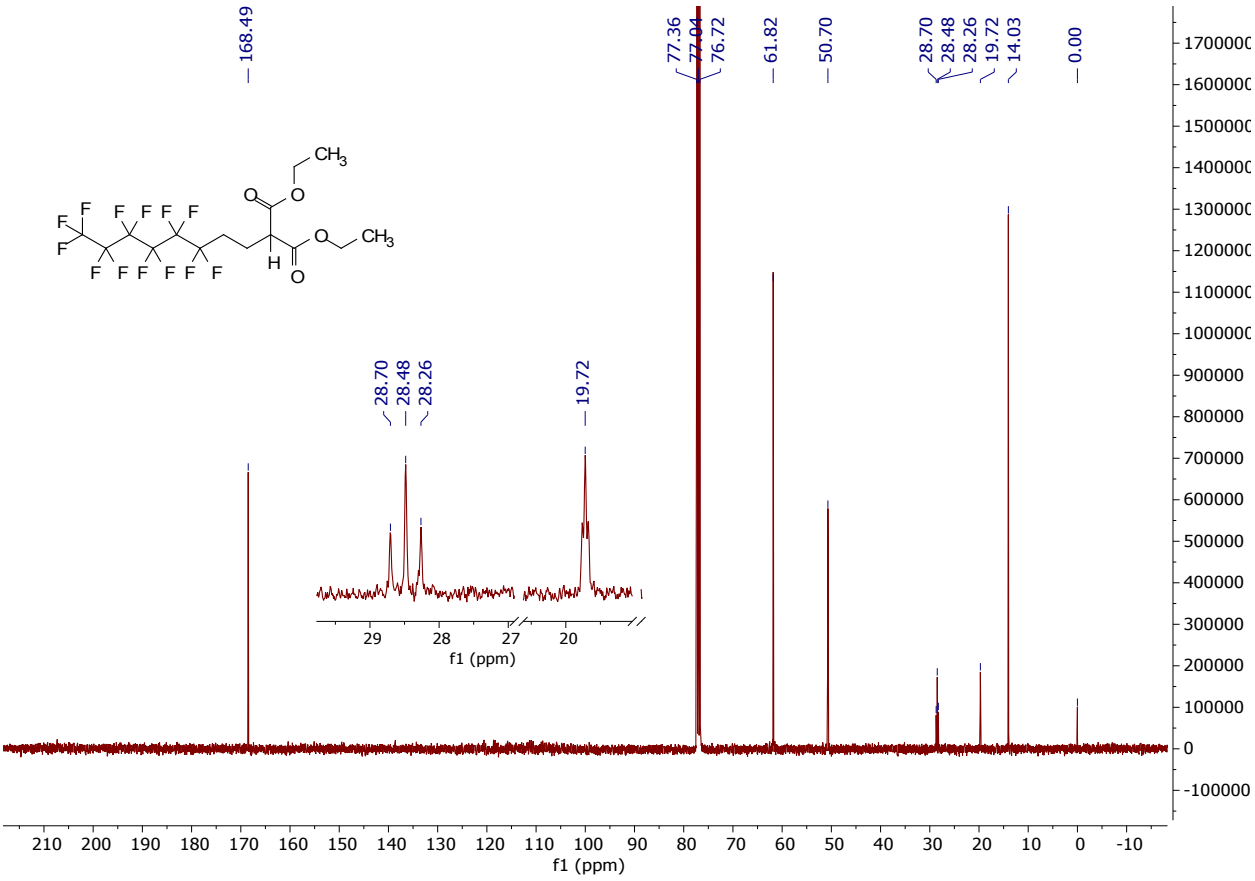

Figure S28. ^{13}C NMR spectrum of compound 3a.

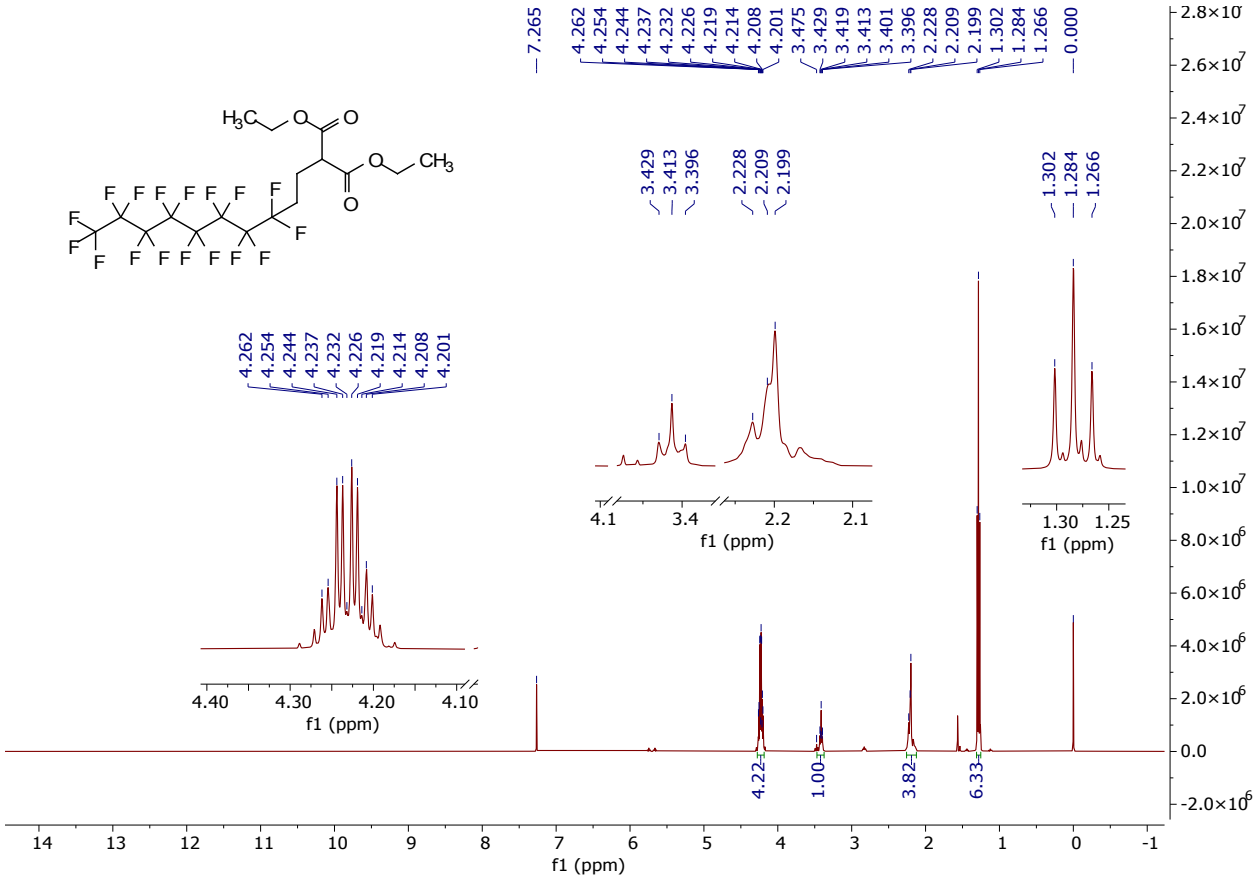

Figure S29. ^{1}H NMR spectrum of compound 3b.

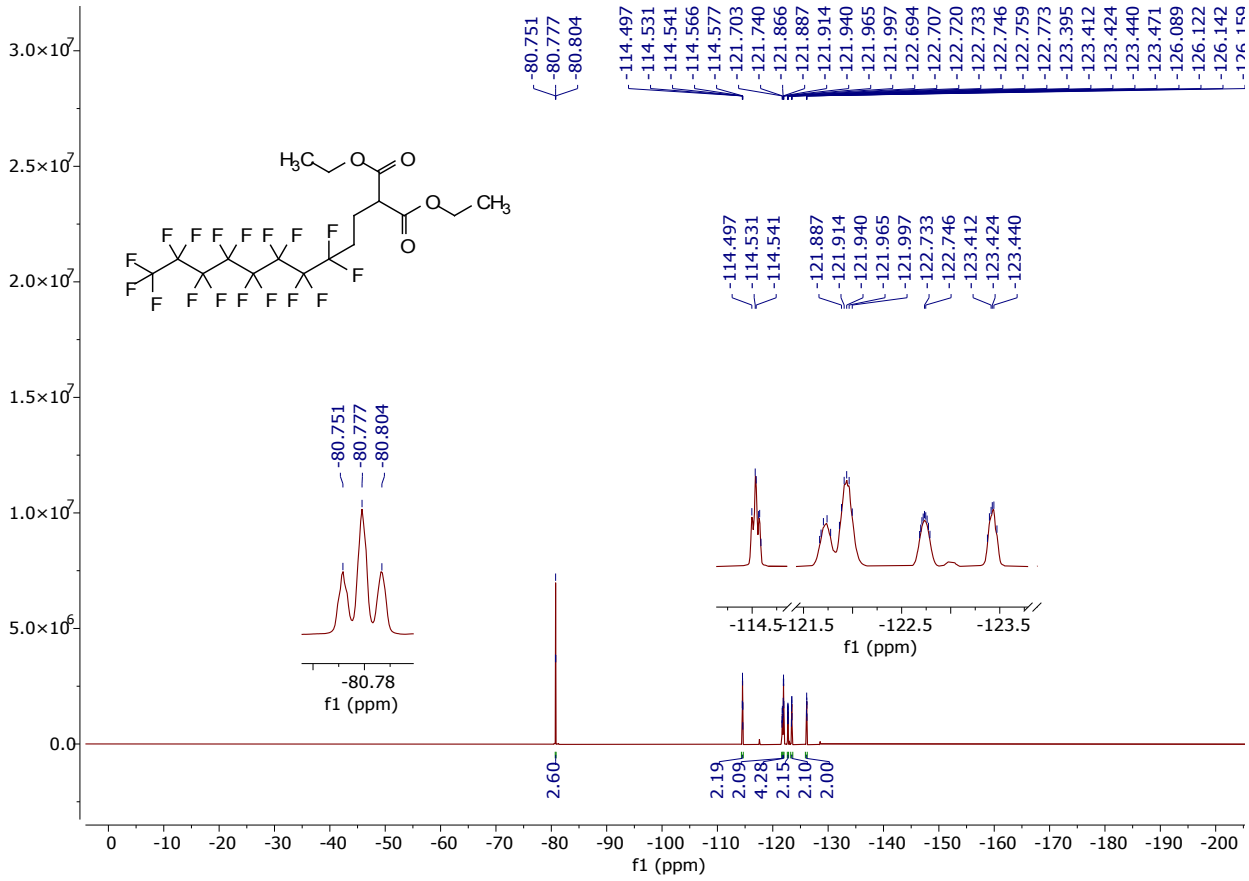

Figure S30. ^{19}F NMR spectrum of compound 3b.

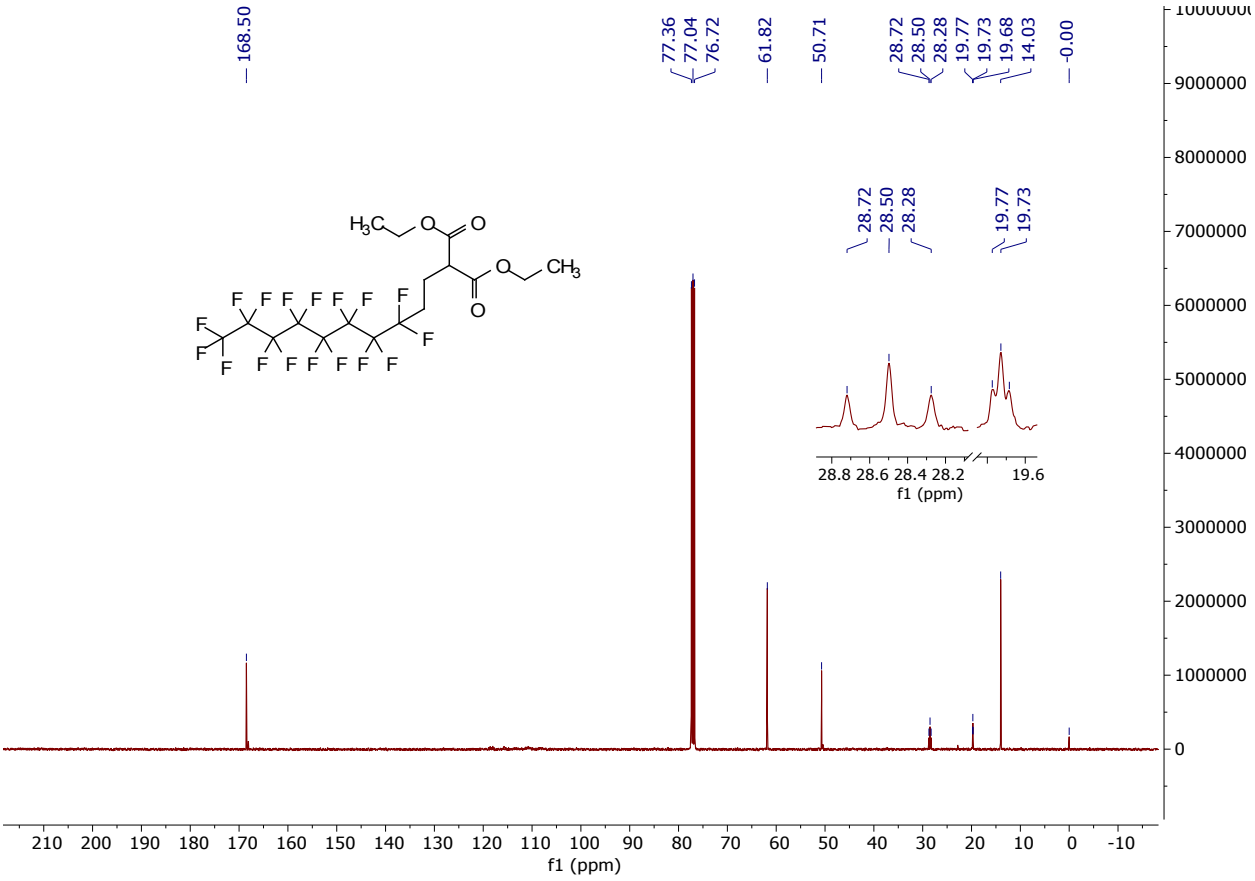

Figure S31. ^{13}C NMR spectrum of compound 3b.

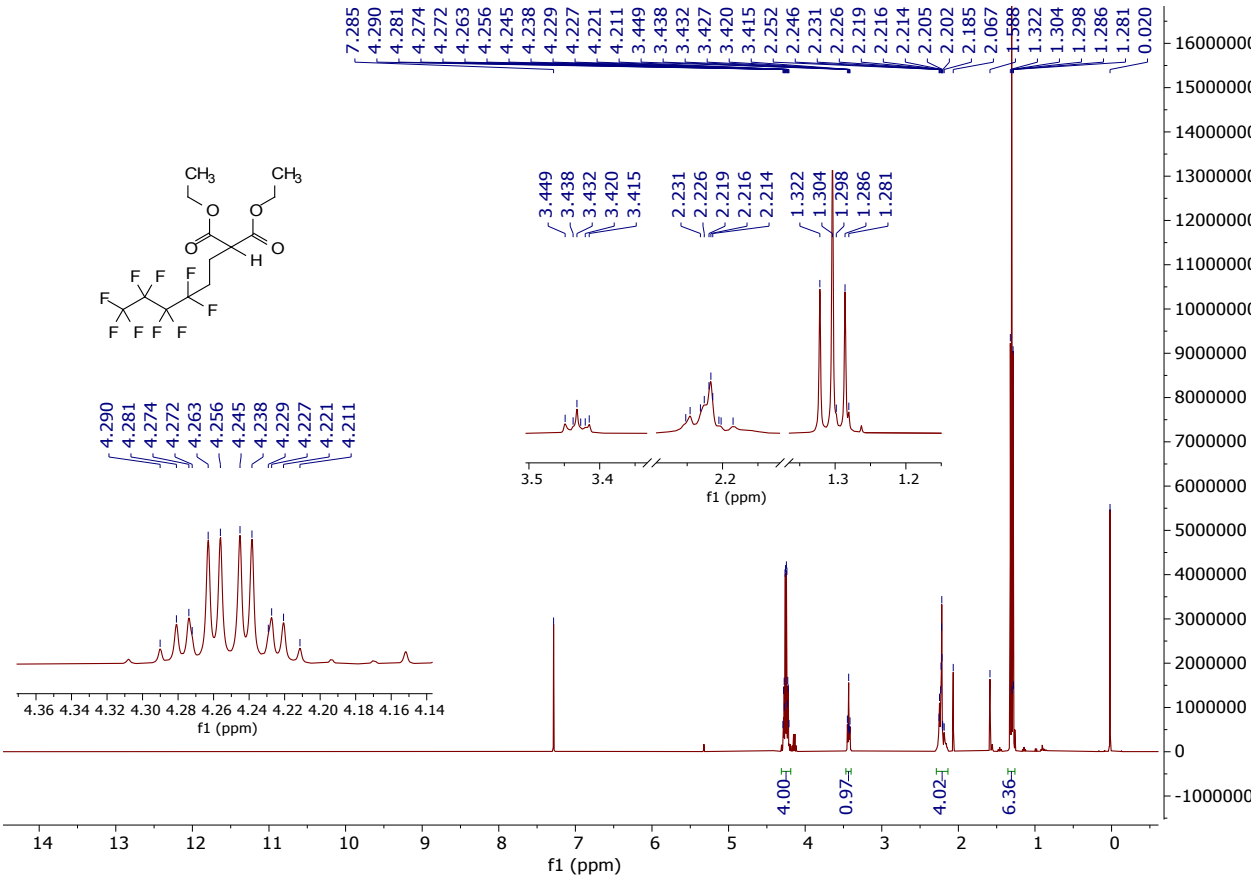

Figure S32. ^{1}H NMR spectrum of compound 3c.

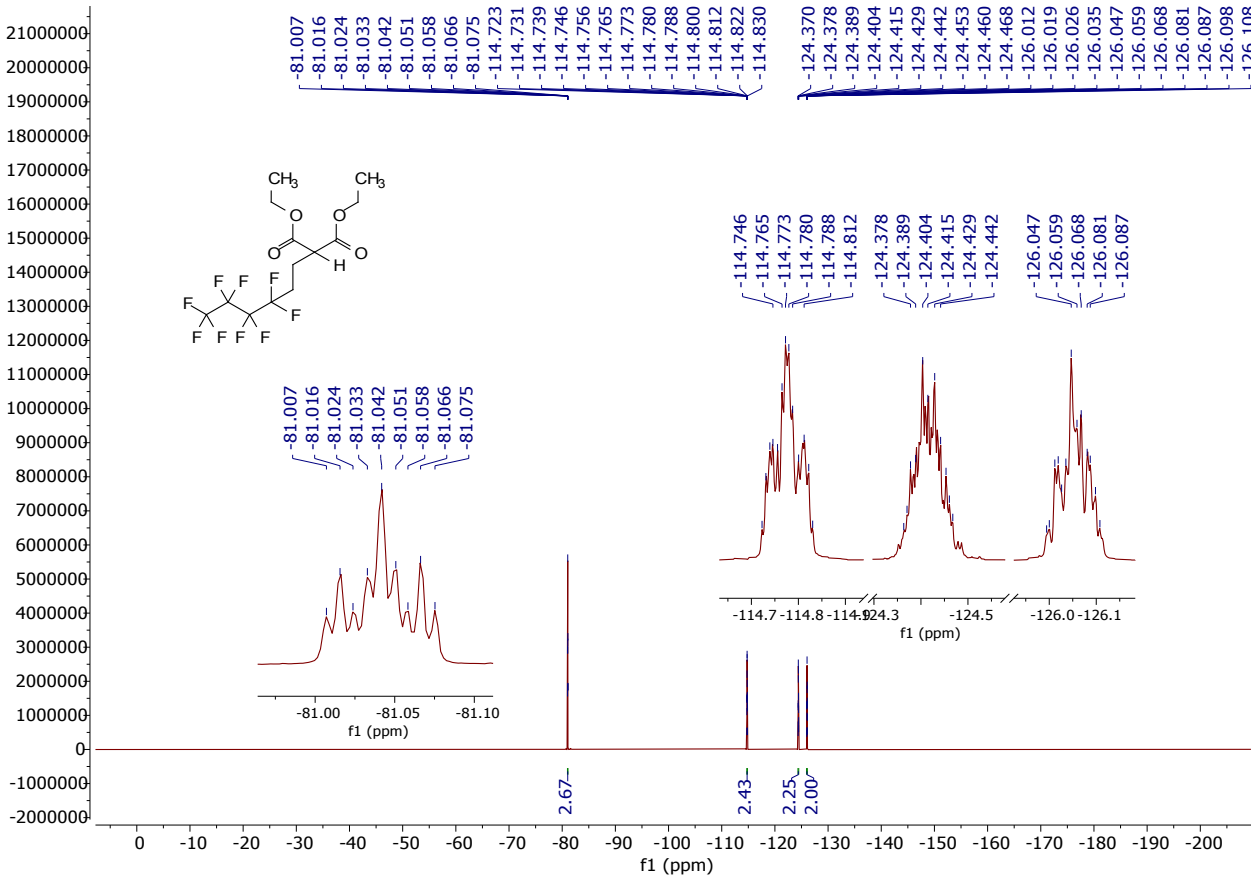

Figure S33. ^{19}F NMR spectrum of compound 3c.

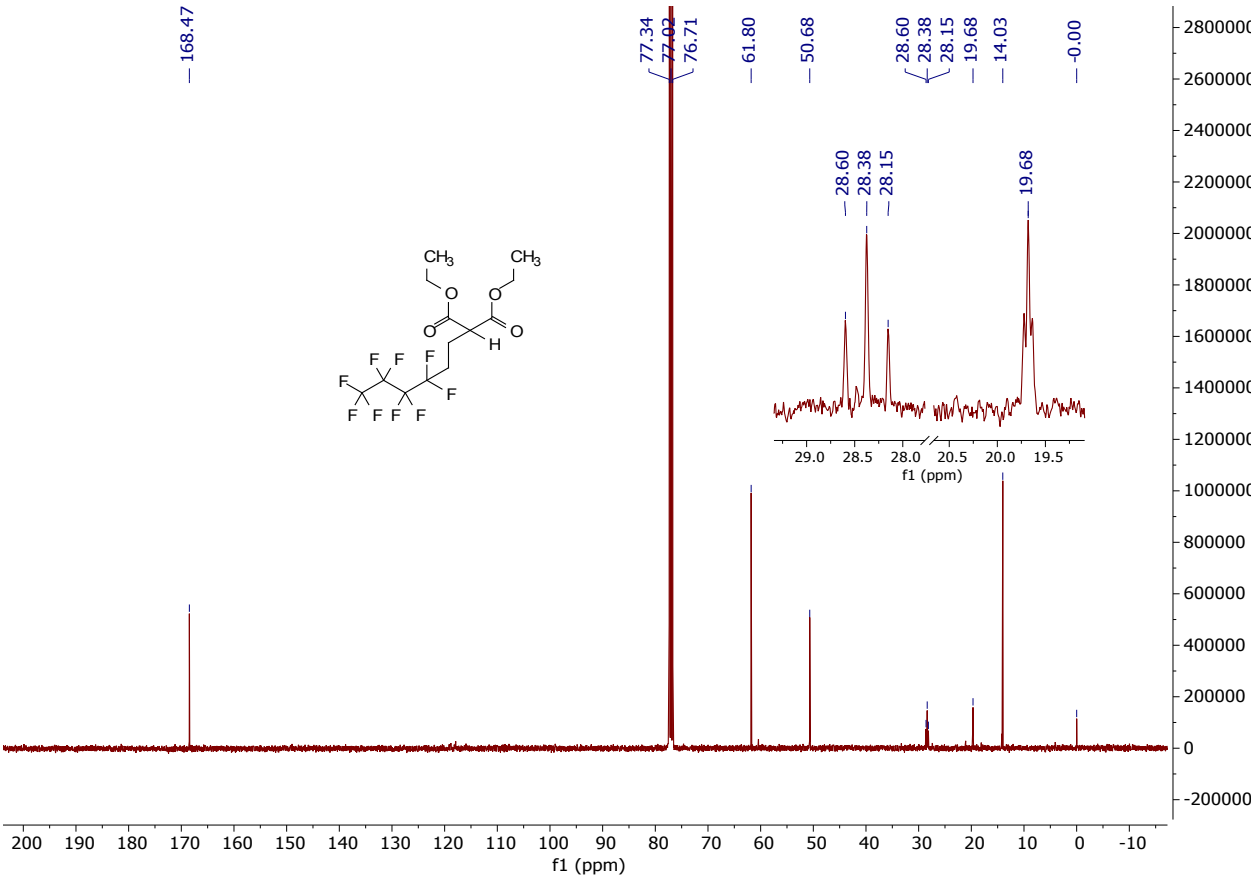

Figure S34. ^{13}C NMR spectrum of compound 3c.

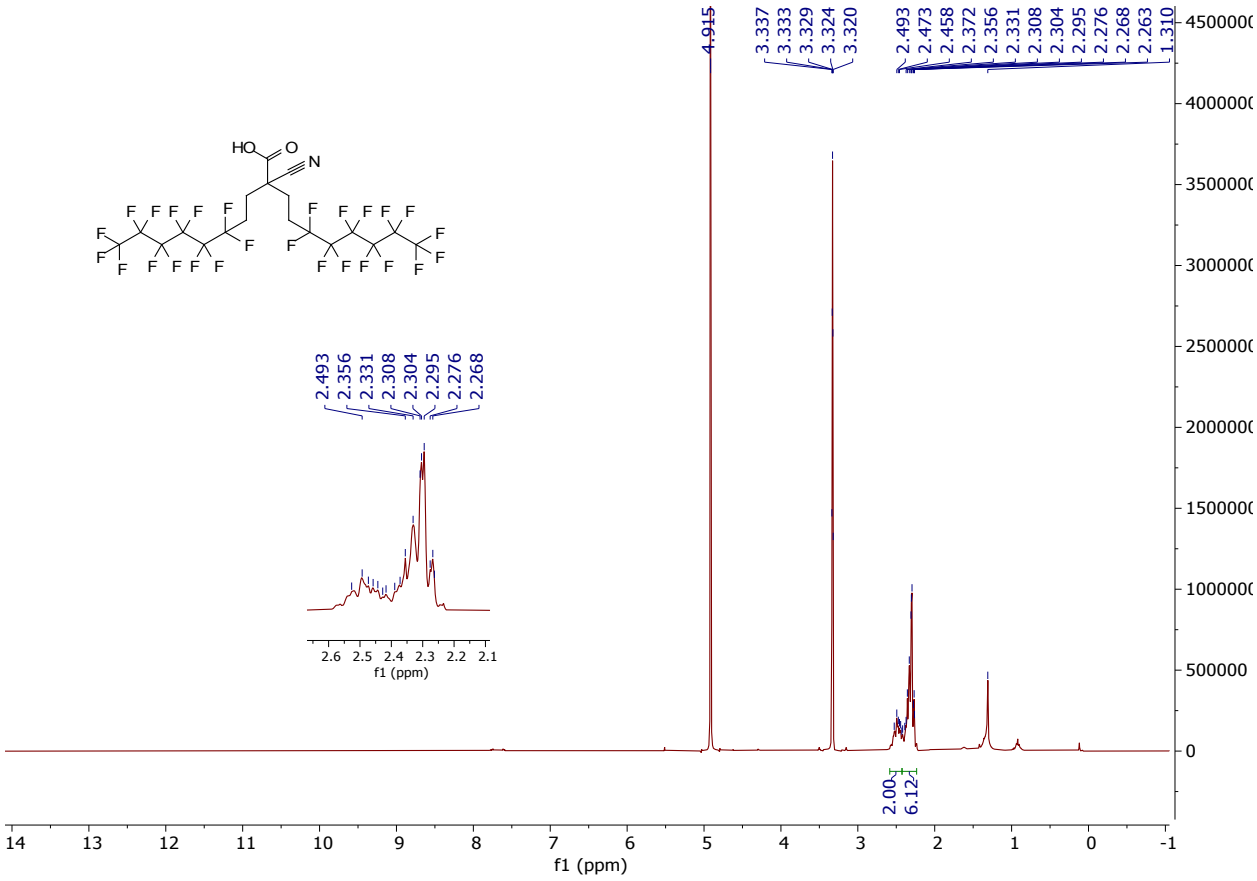

Figure S35. ^{1}H NMR spectrum of PD-6.

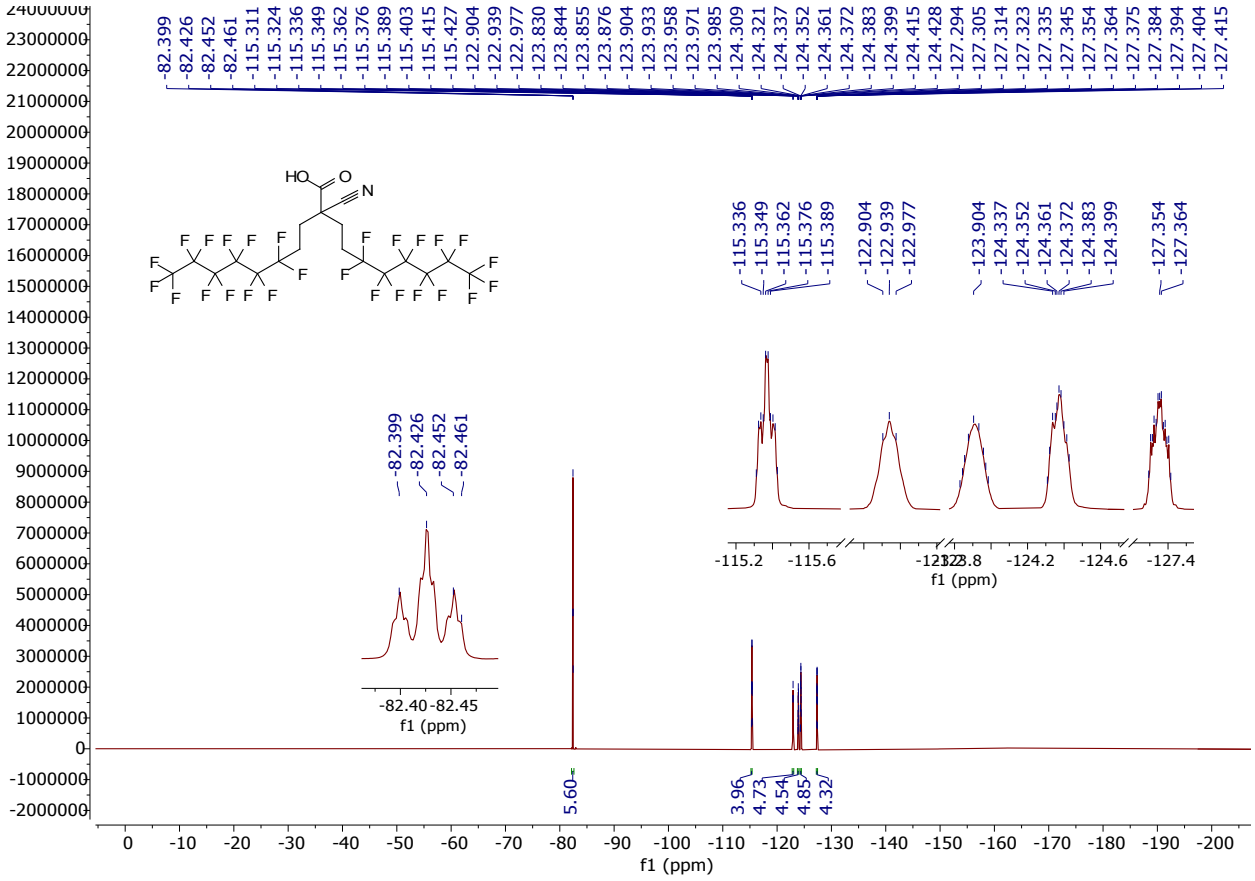

Figure S36. ^{19}F NMR spectrum of PD-6.

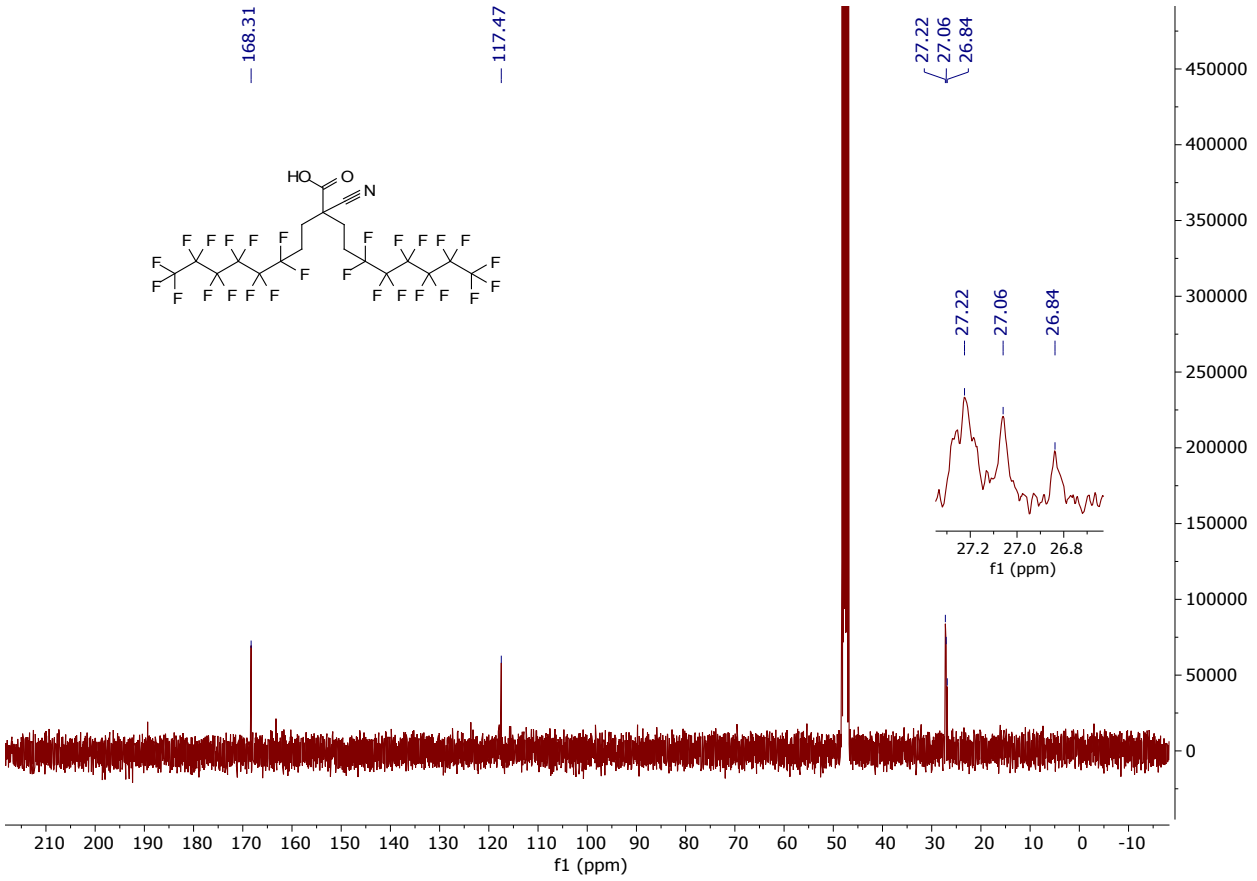

Figure S37. ^{13}C NMR spectrum of PD-6.

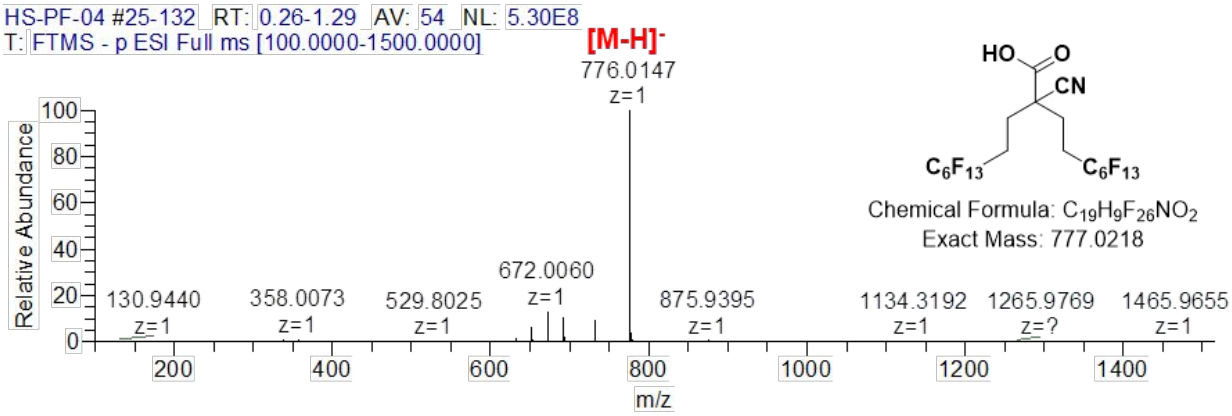

Figure S38. High resolution mass spectrum of PD-6.

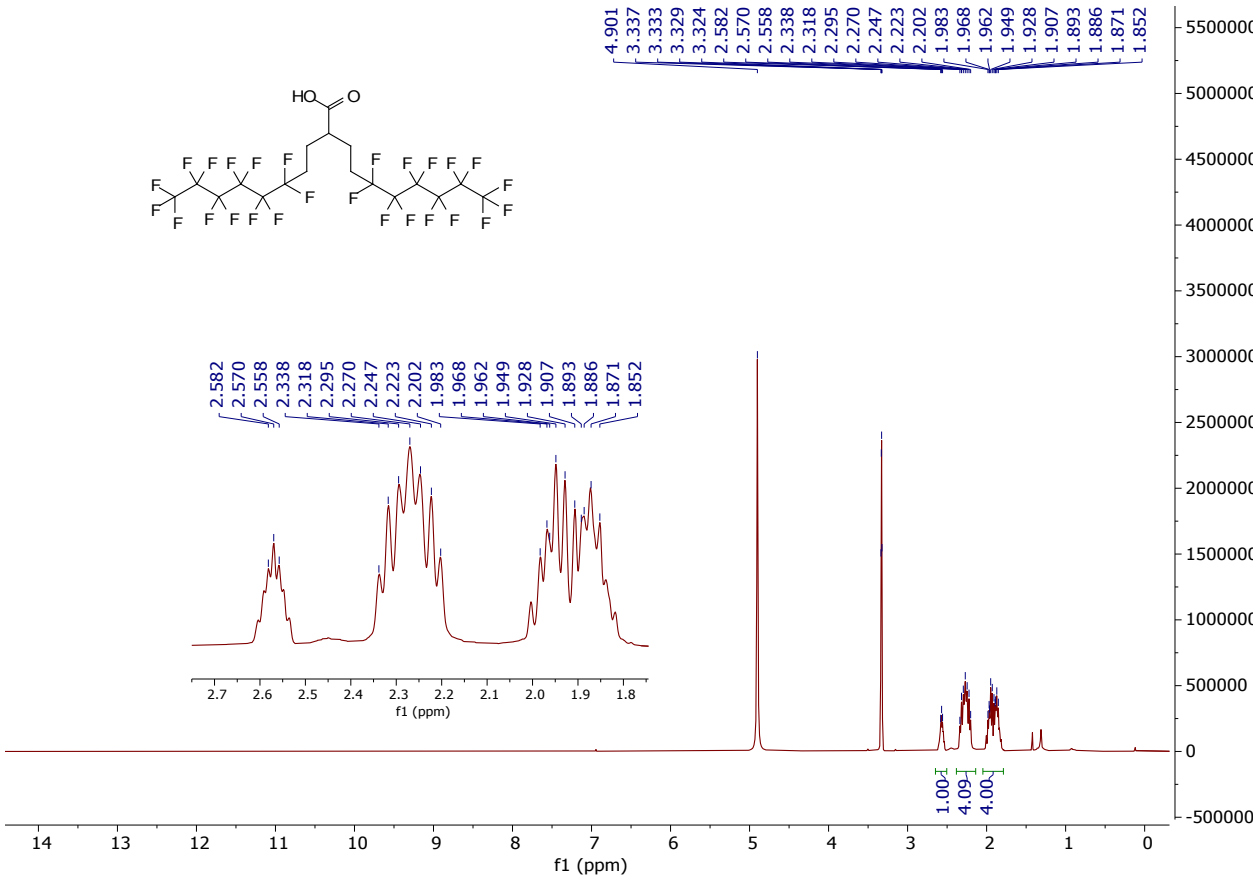

Figure S39. ^{1}H NMR spectrum of PD-7.

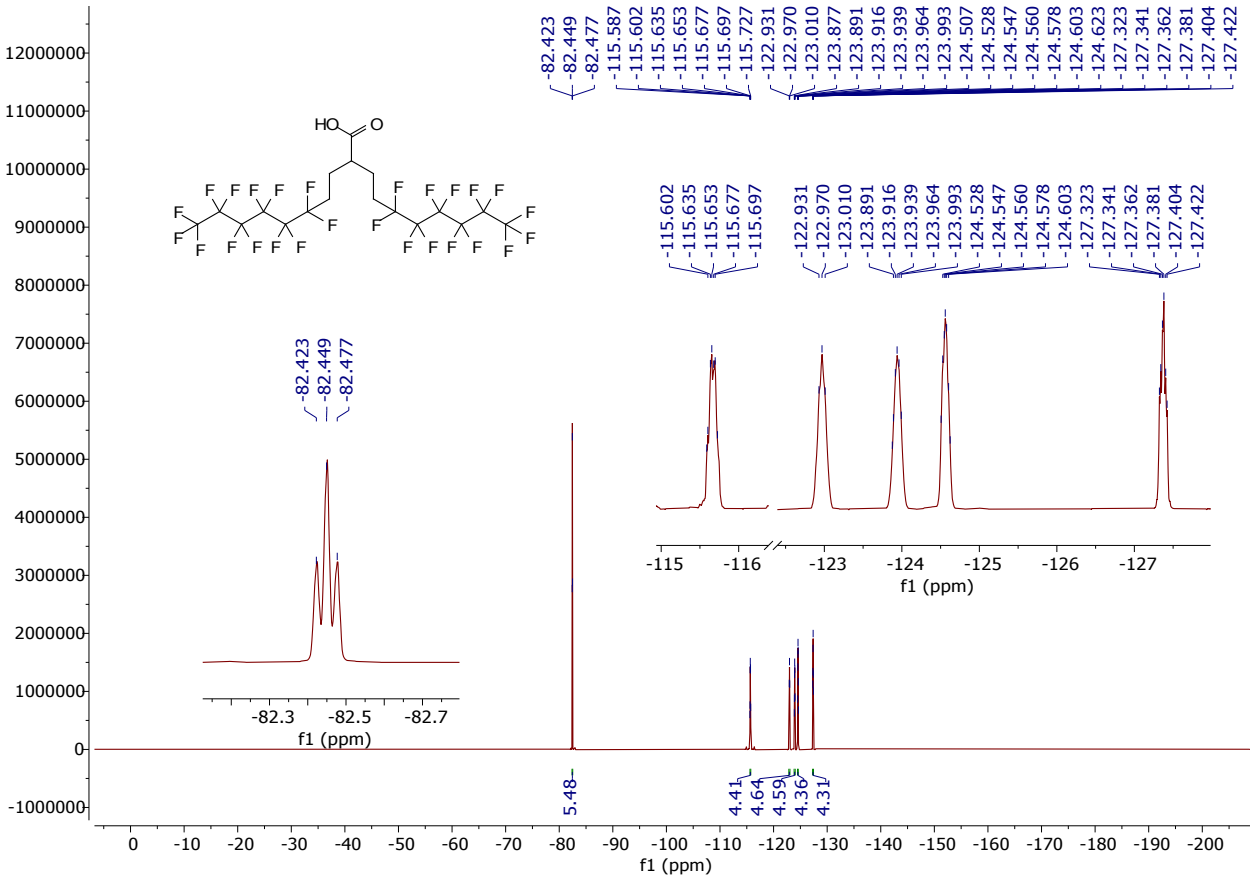

Figure S40. ^{19}F NMR spectrum of PD-7.

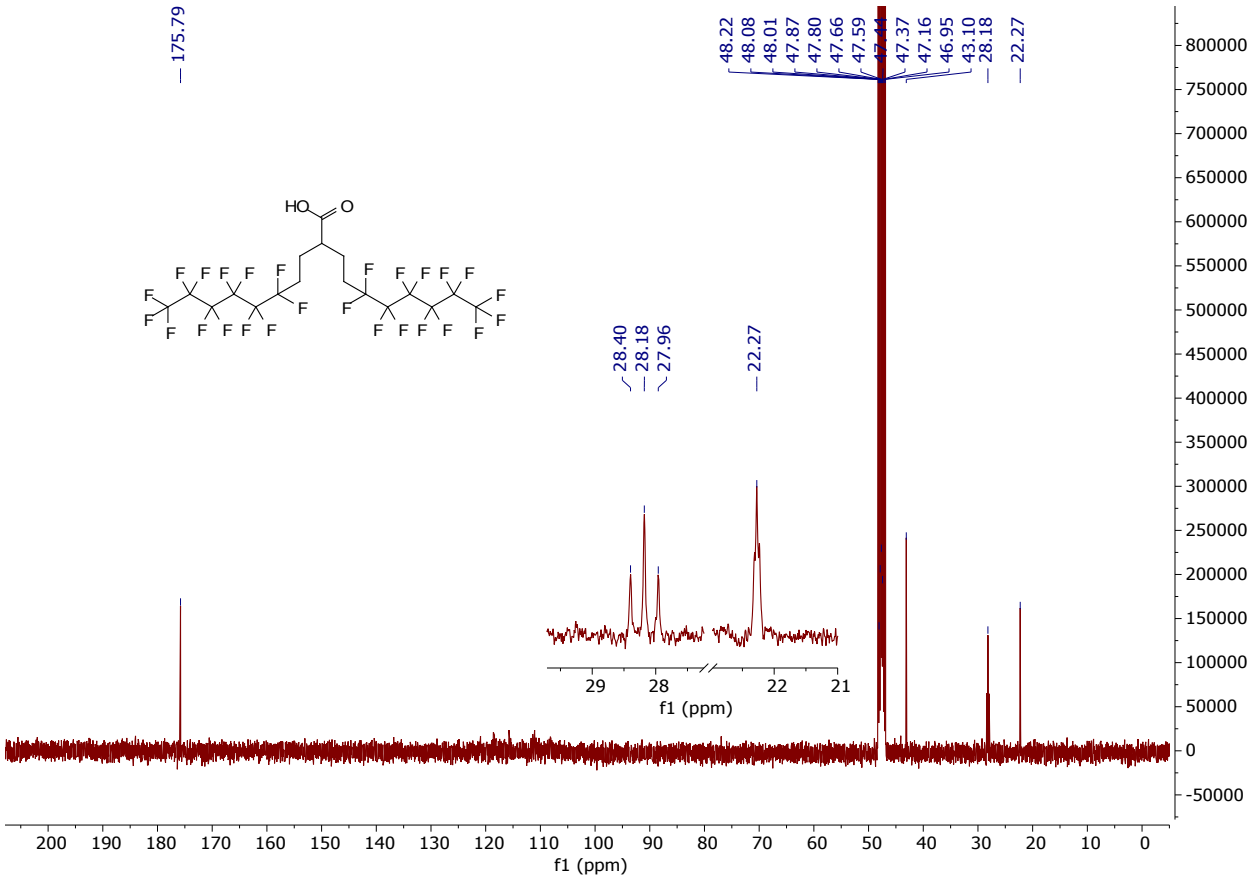

Figure S41. ^{13}C NMR spectrum of PD-7.

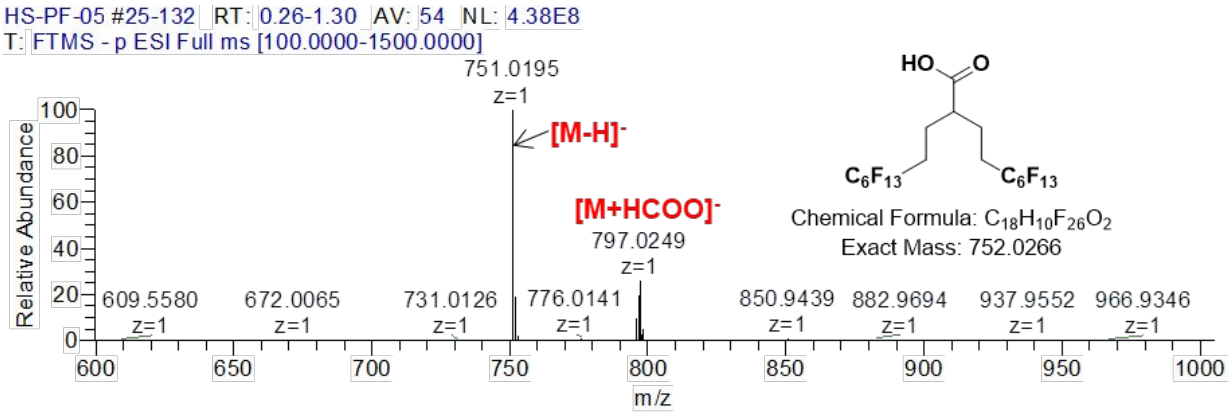

Figure S42. High resolution mass spectrum of PD-7.

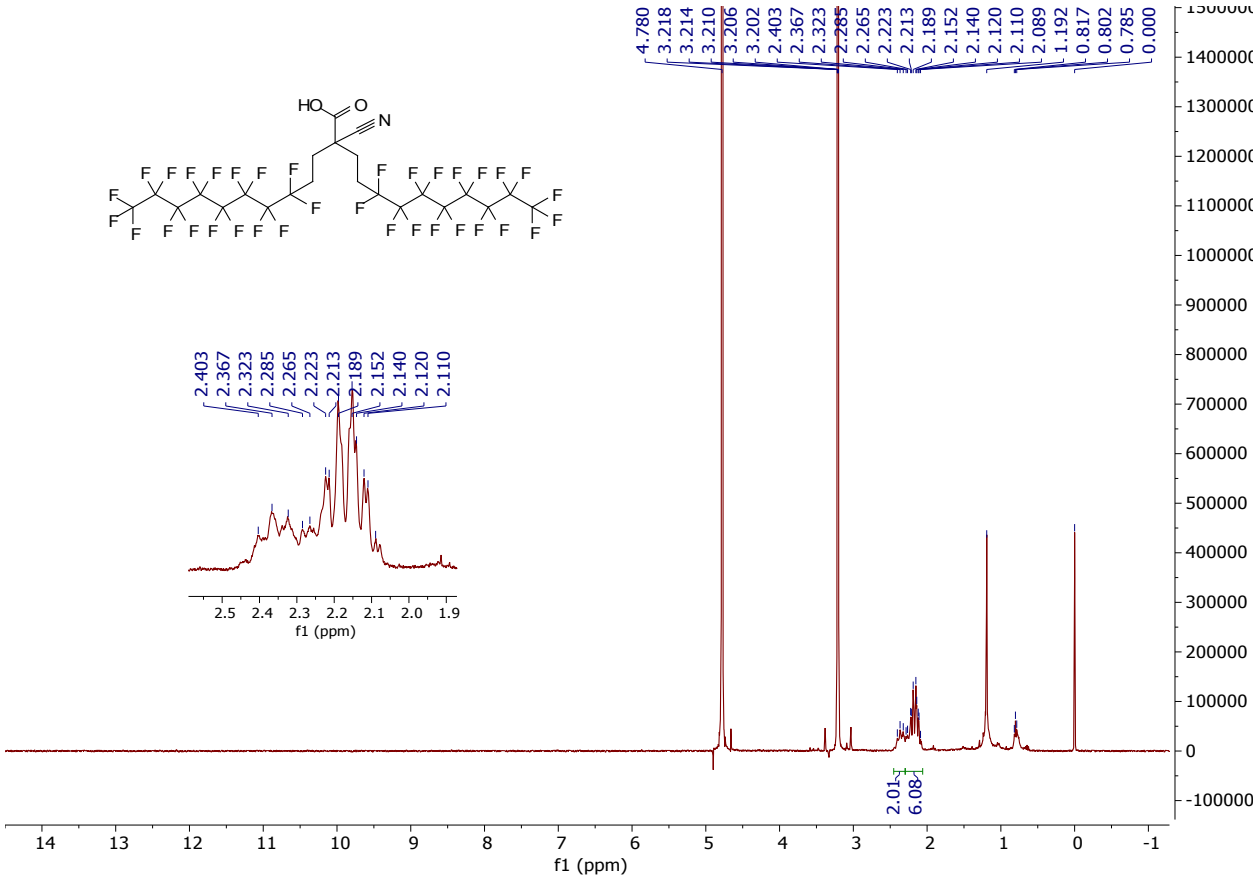

Figure S43. ^{1}H NMR spectrum of PD-8.

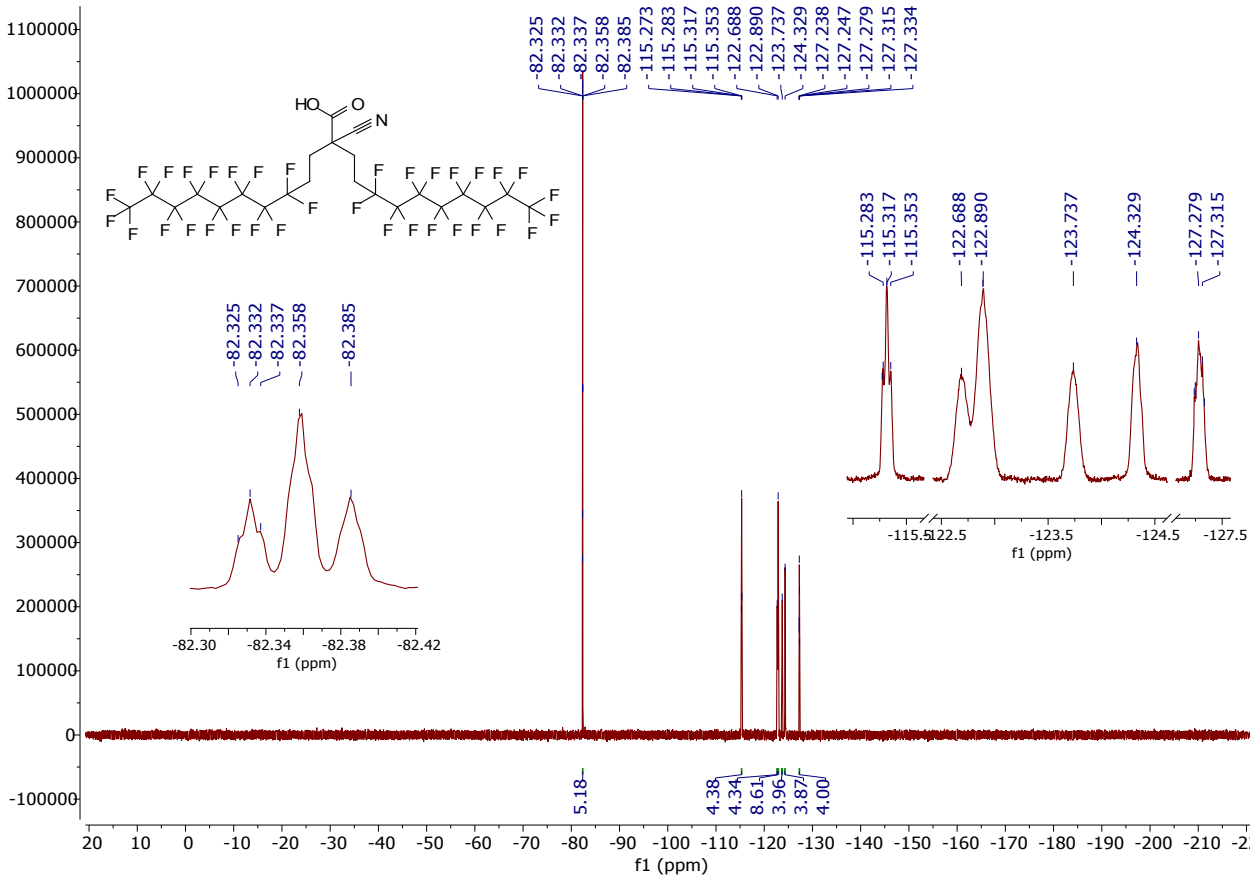

Figure S44. ^{19}F NMR spectrum of PD-8.

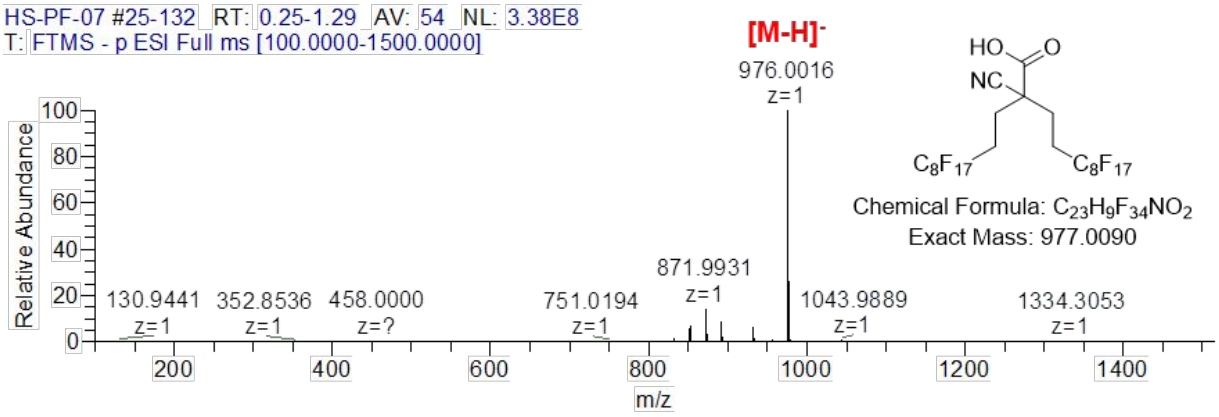

Figure S45. High resolution mass spectrum of PD-8.

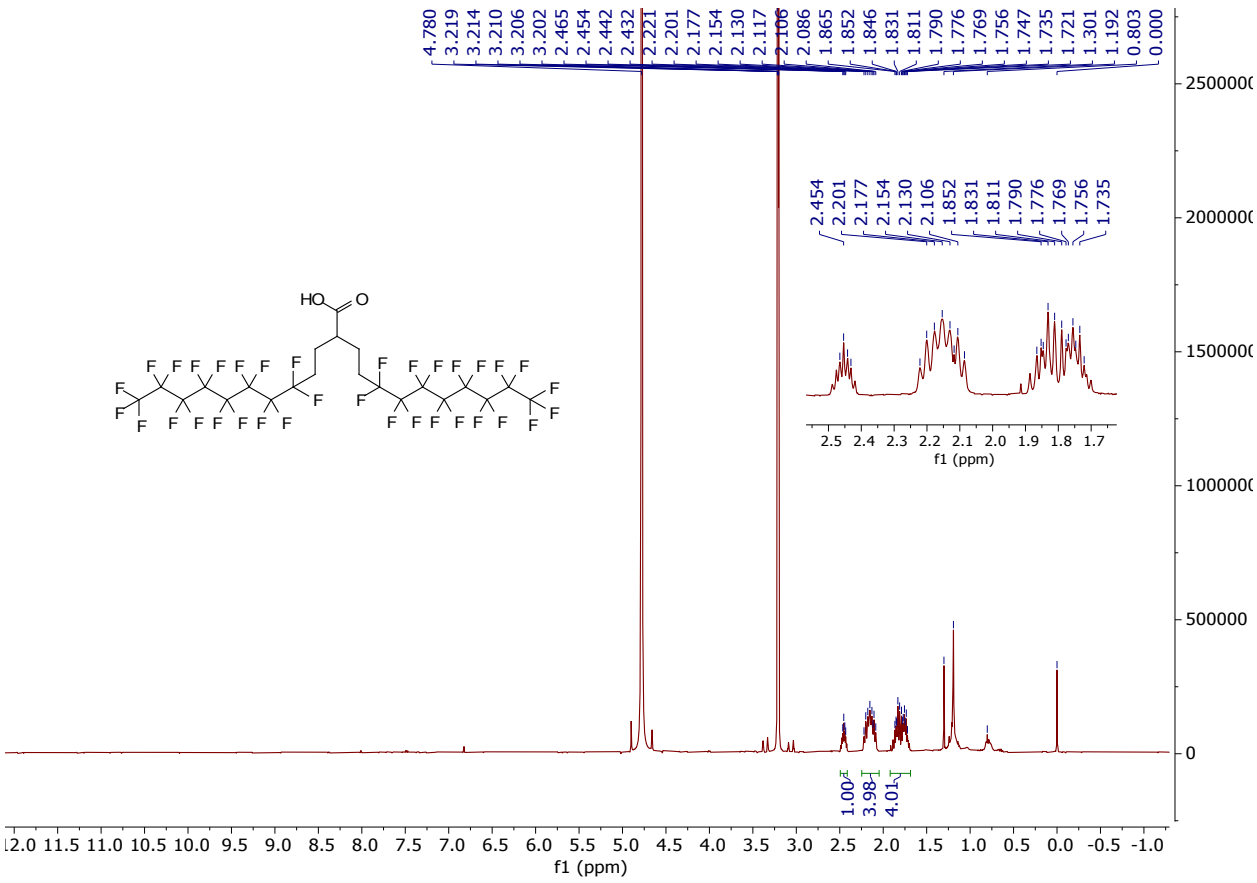

Figure S46. ^{1}H NMR spectrum of PD-9.

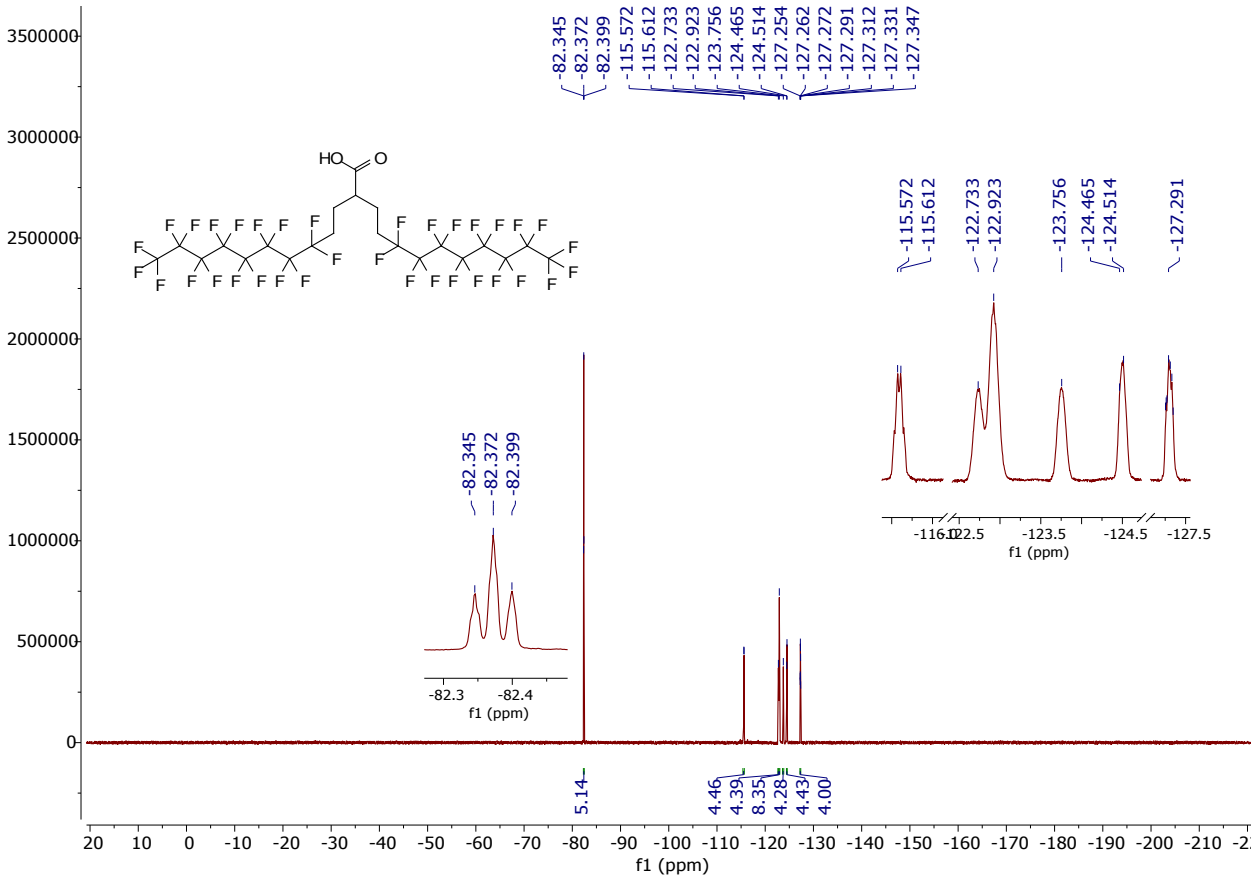

Figure S47. ^{19}F NMR spectrum of PD-9.

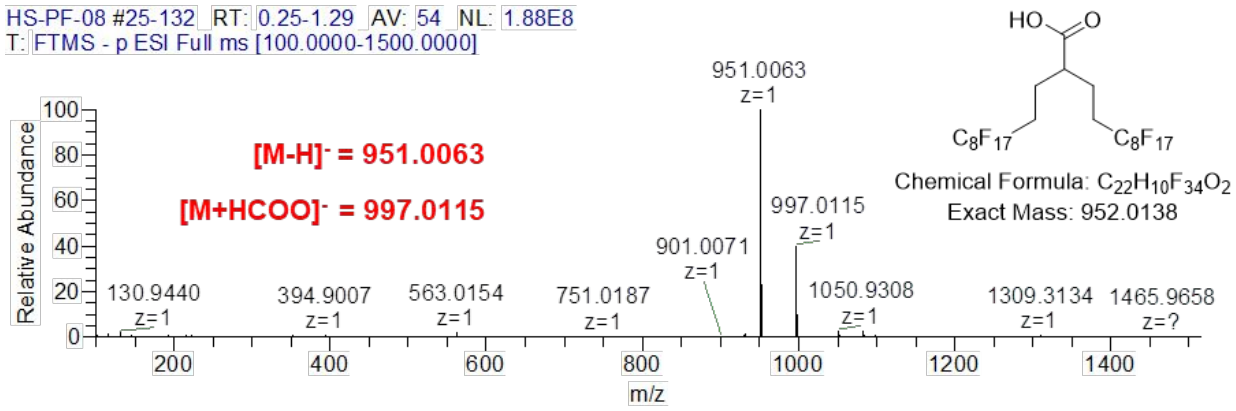

Figure S48. High resolution mass spectrum of PD-9.

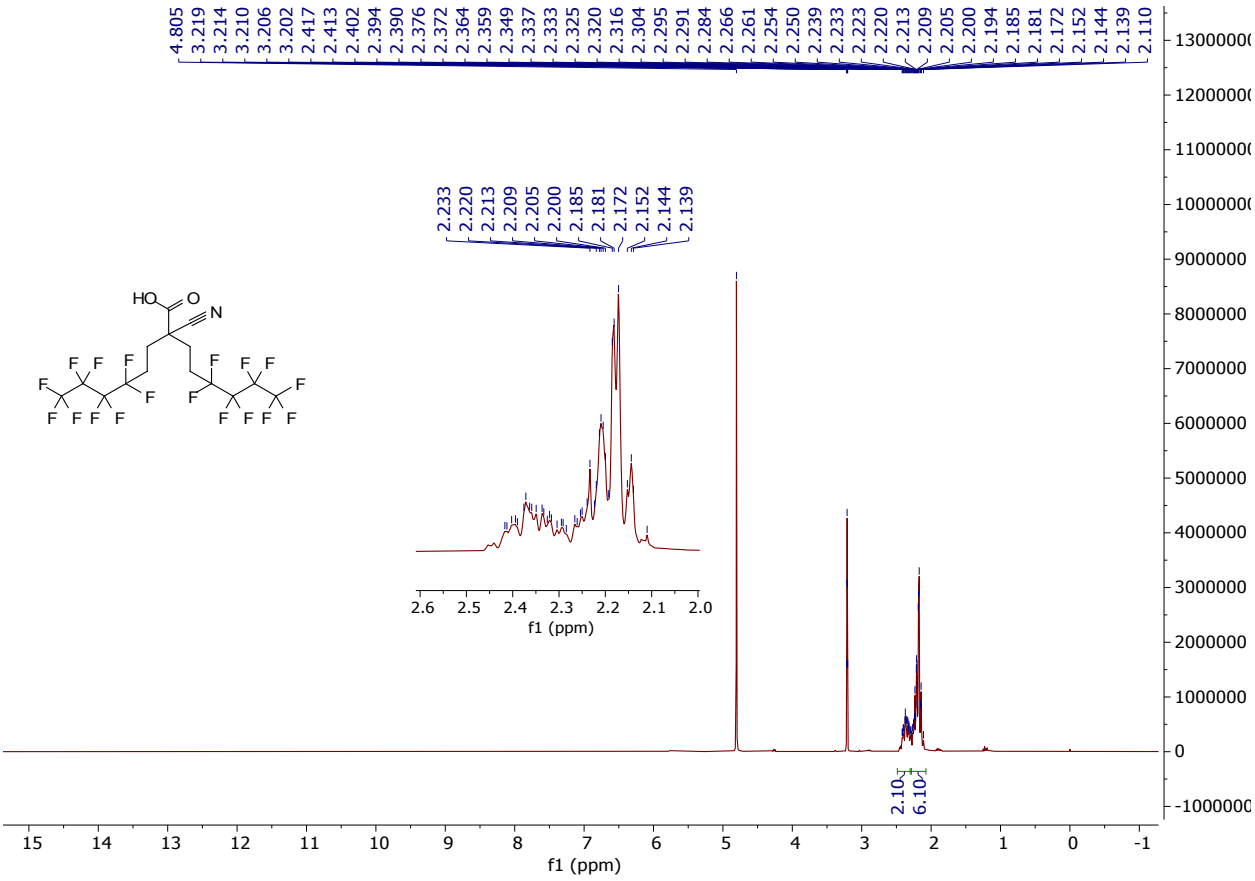

Figure S49. ^{1}H NMR spectrum of PD-10.

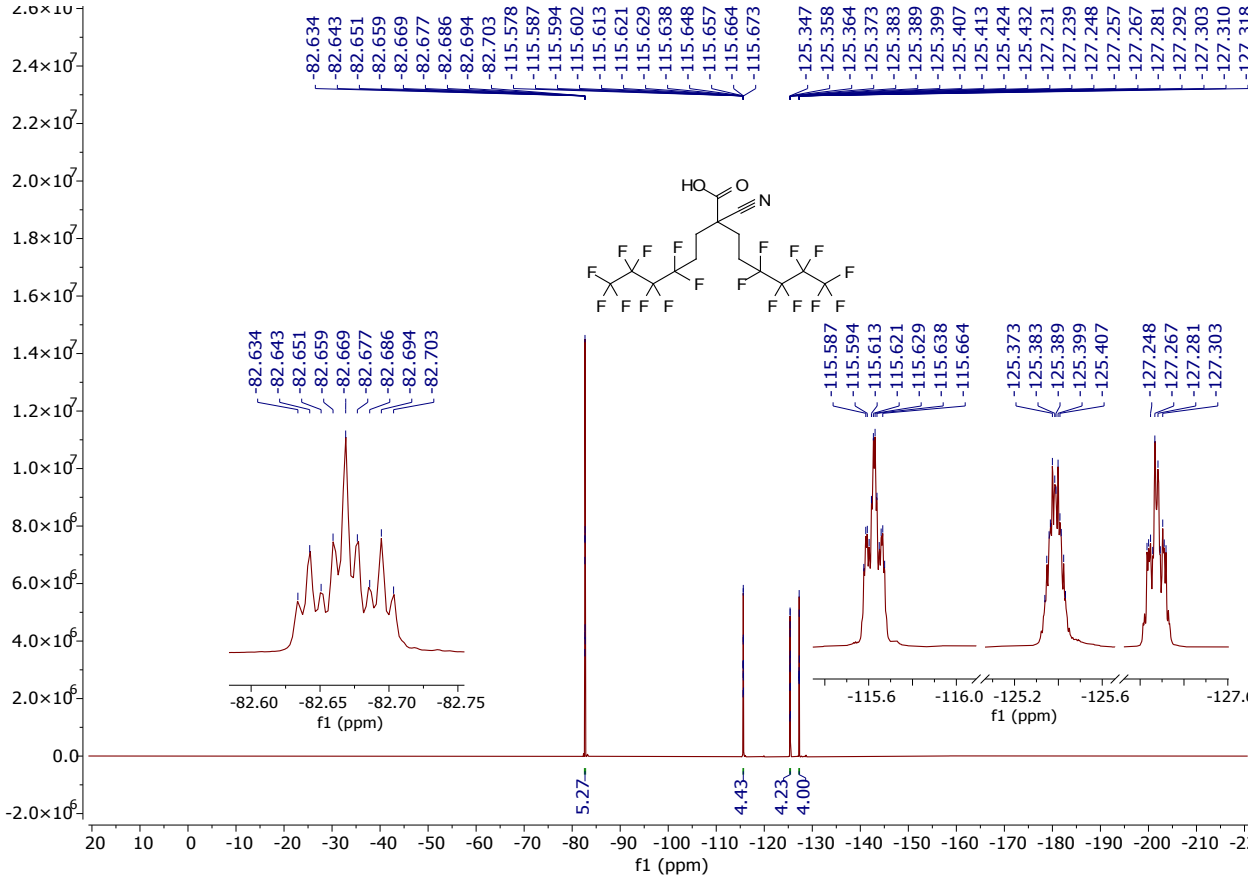

Figure S50. ^{19}F NMR spectrum of PD-10.

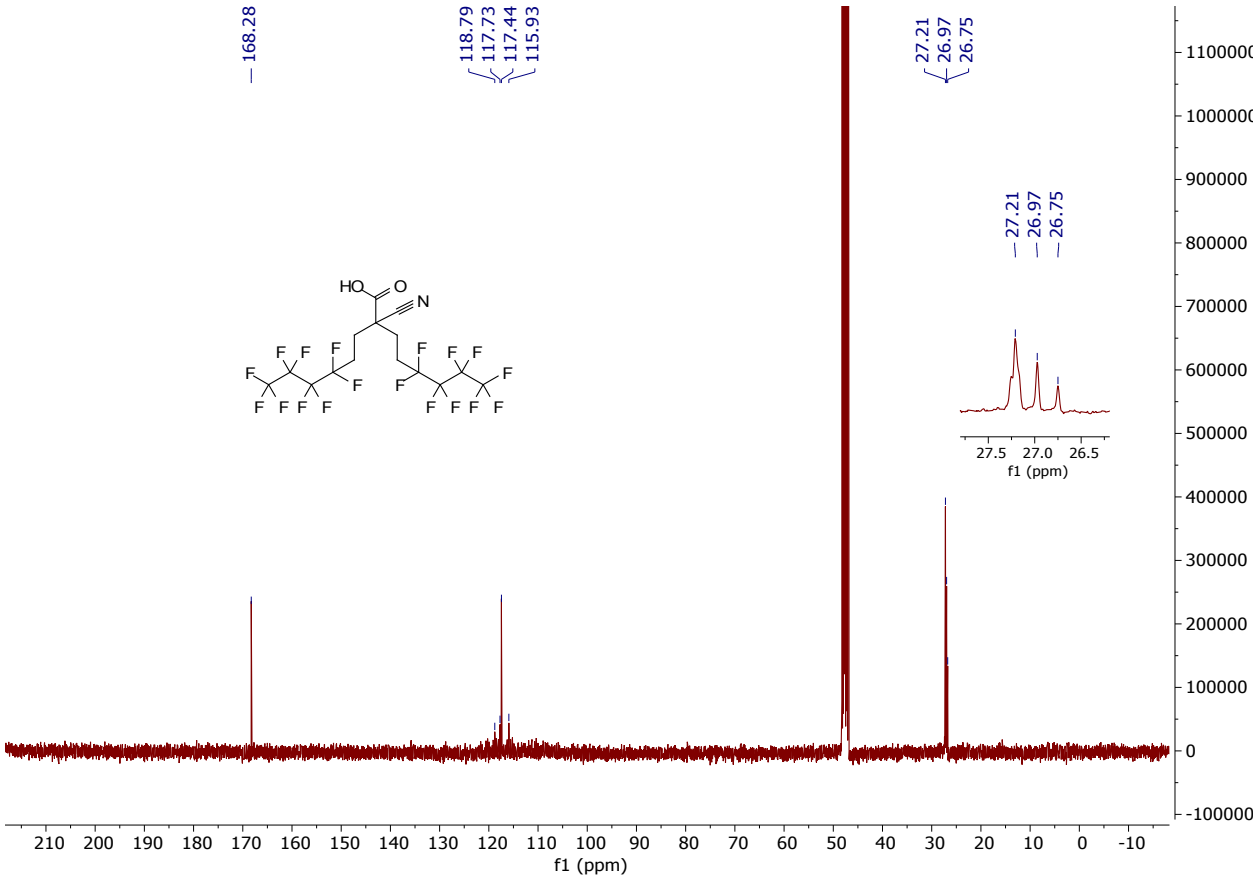

Figure S51. ^{13}C NMR spectrum of PD-10.

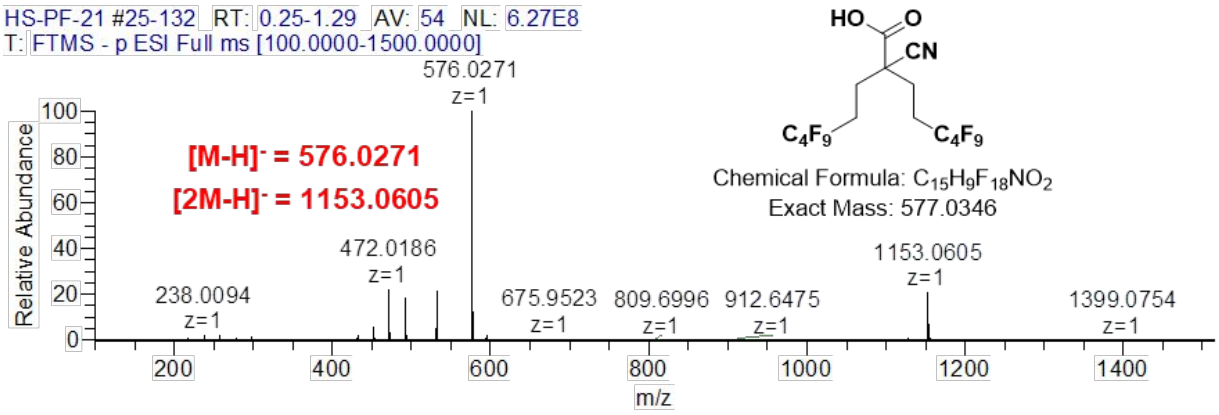

Figure S52. High resolution mass spectrum of PD-10.

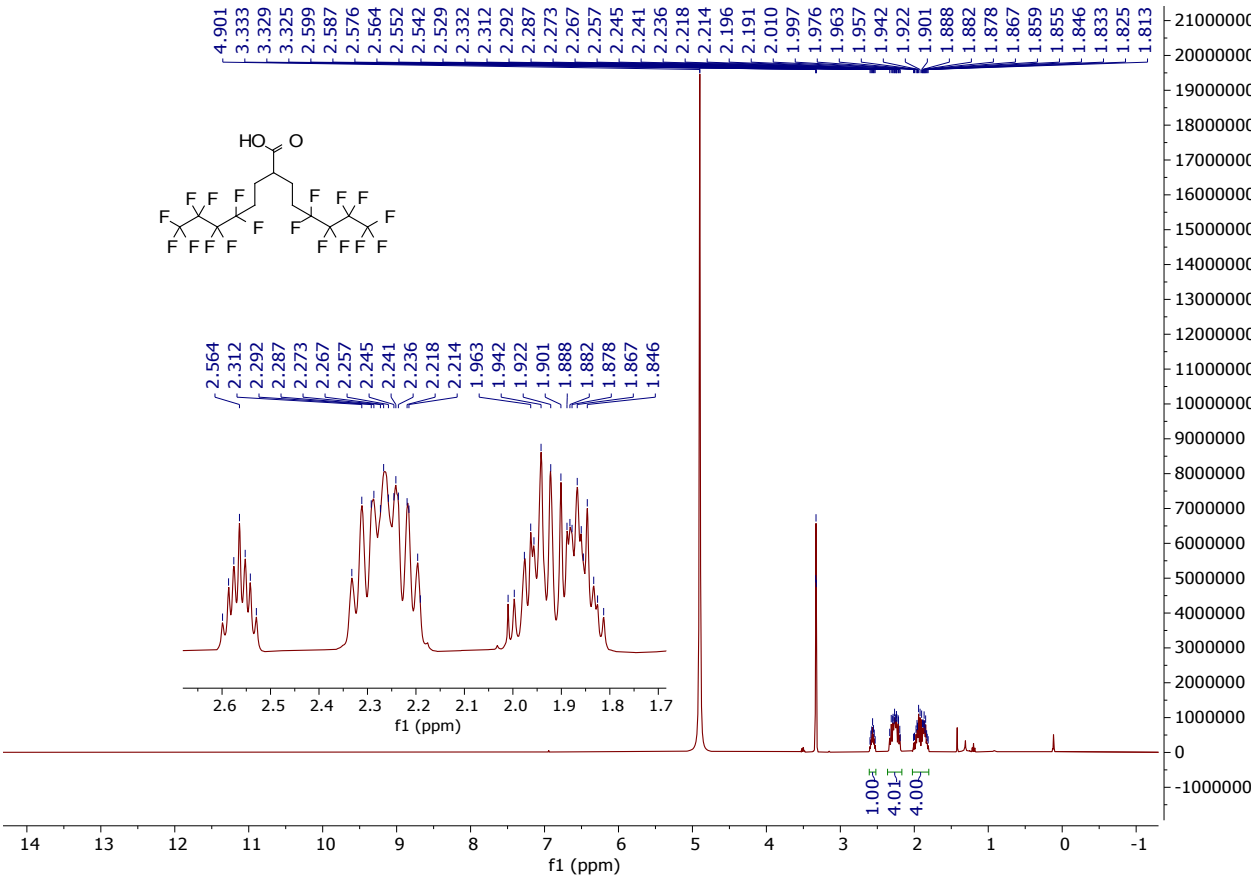

Figure S53. ^{1}H NMR spectrum of PD-11.

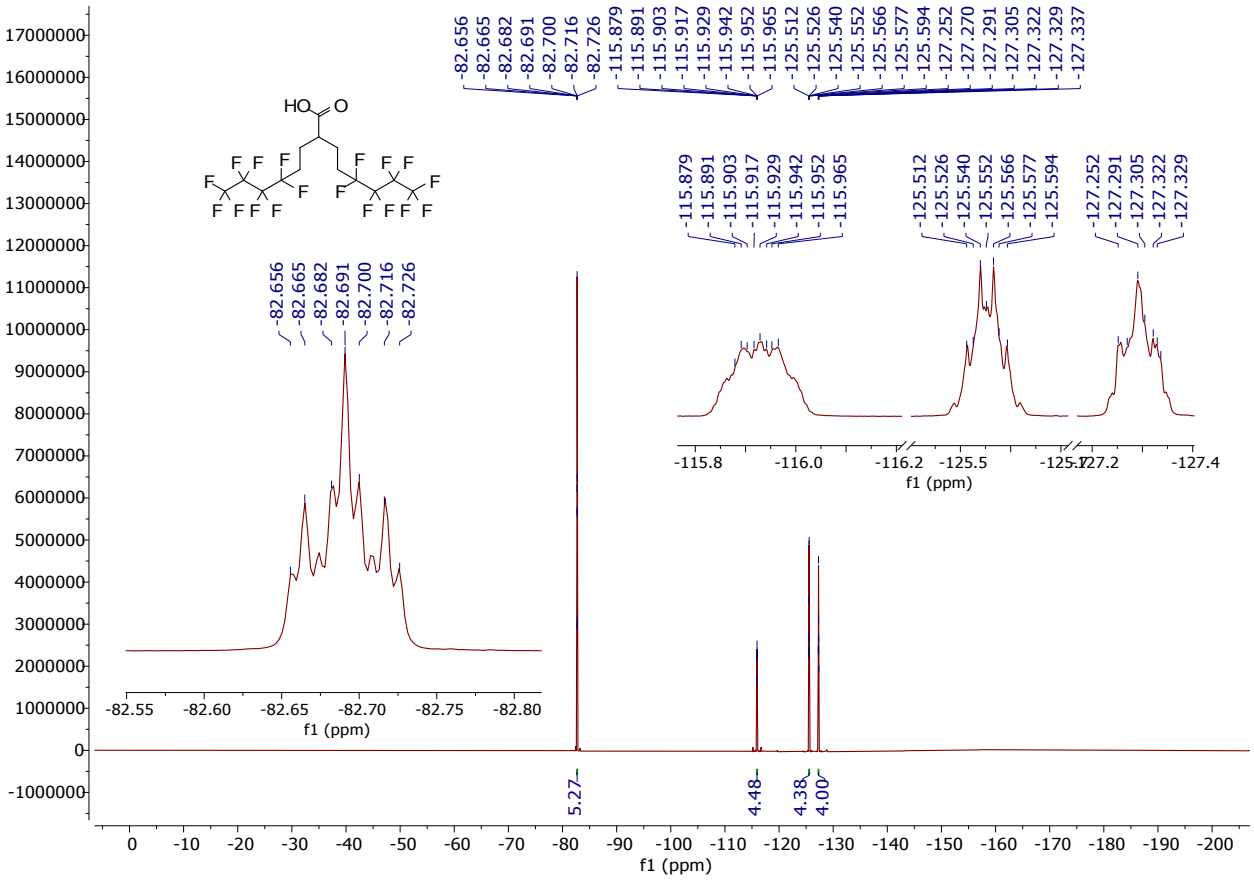

Figure S54. ^{19}F NMR spectrum of PD-11.

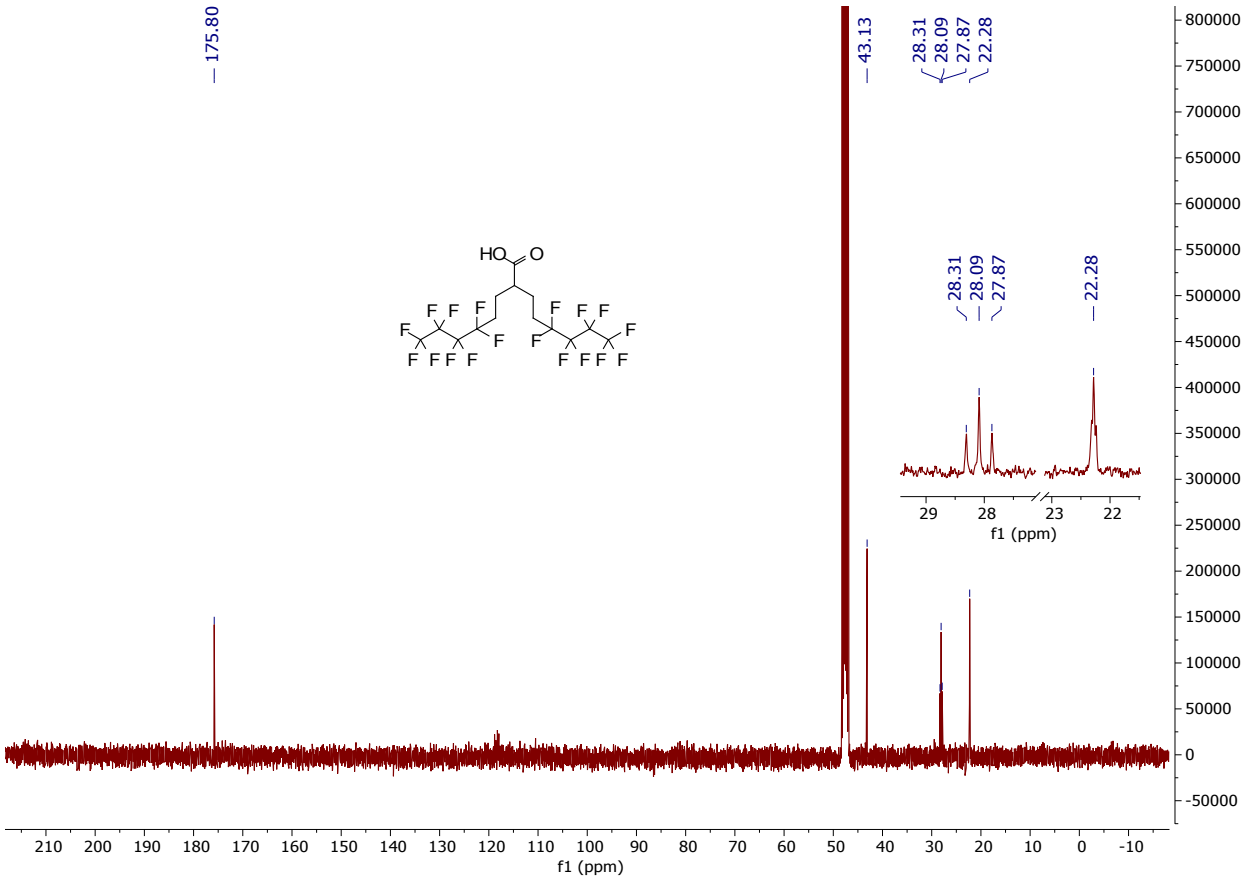

Figure S55. ^{13}C NMR spectrum of PD-11.

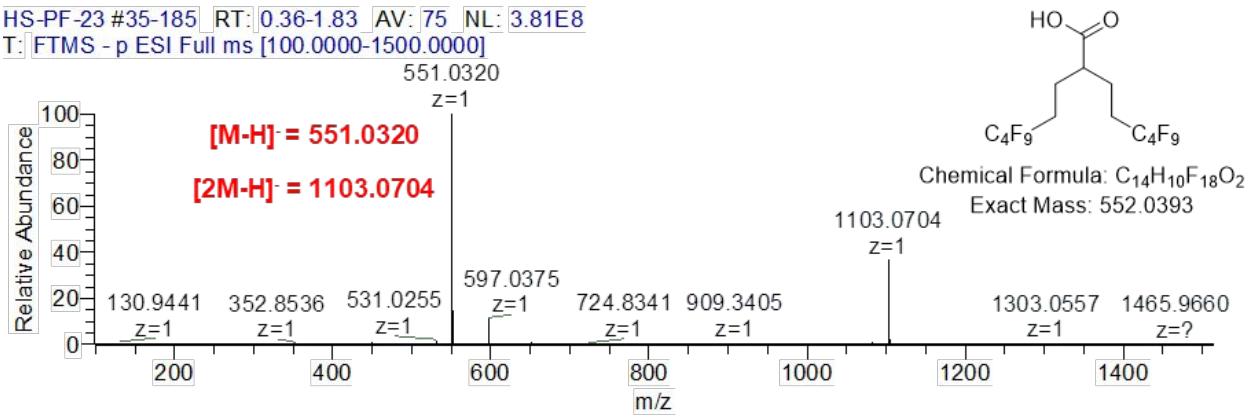

Figure S56. High resolution mass spectrum of PD-11.

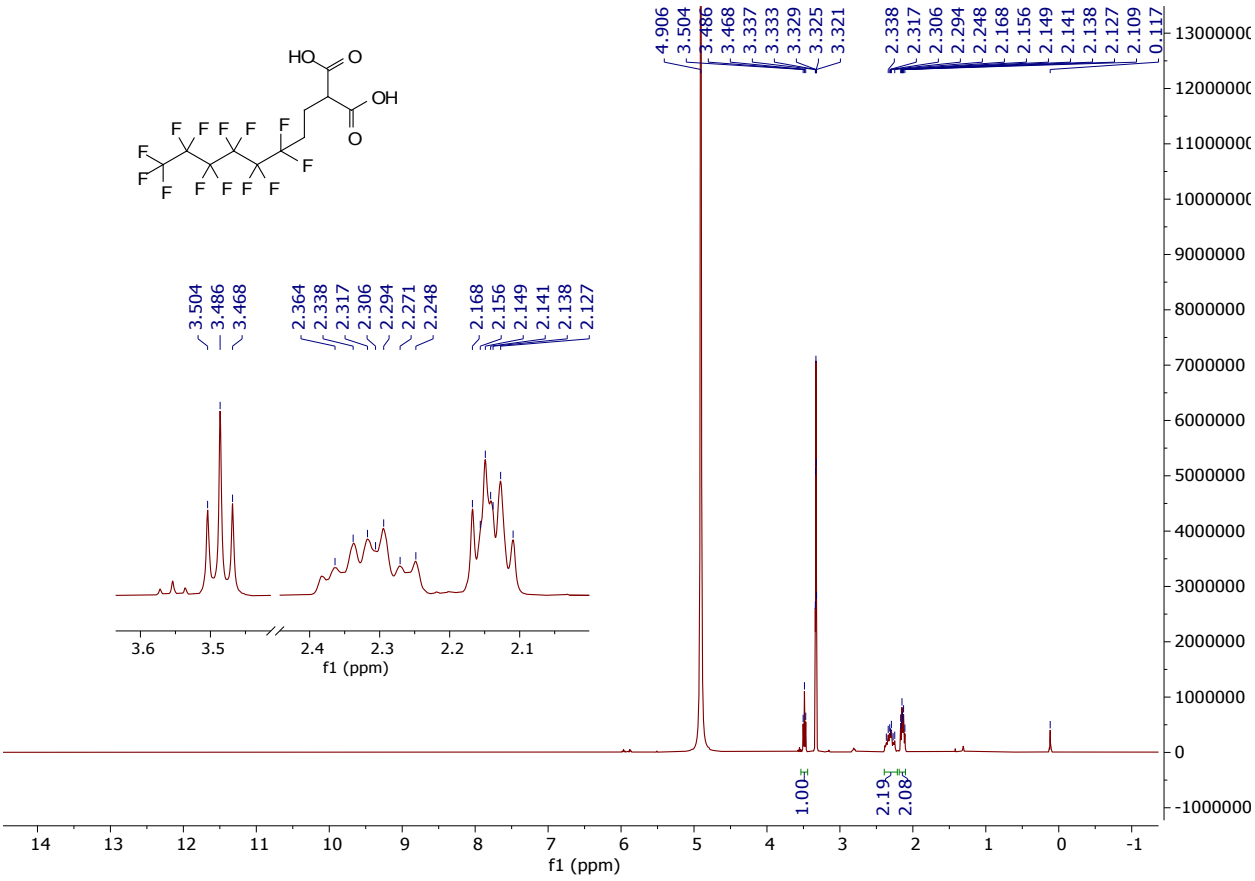

Figure S57. ^{1}H NMR spectrum of PD-12.

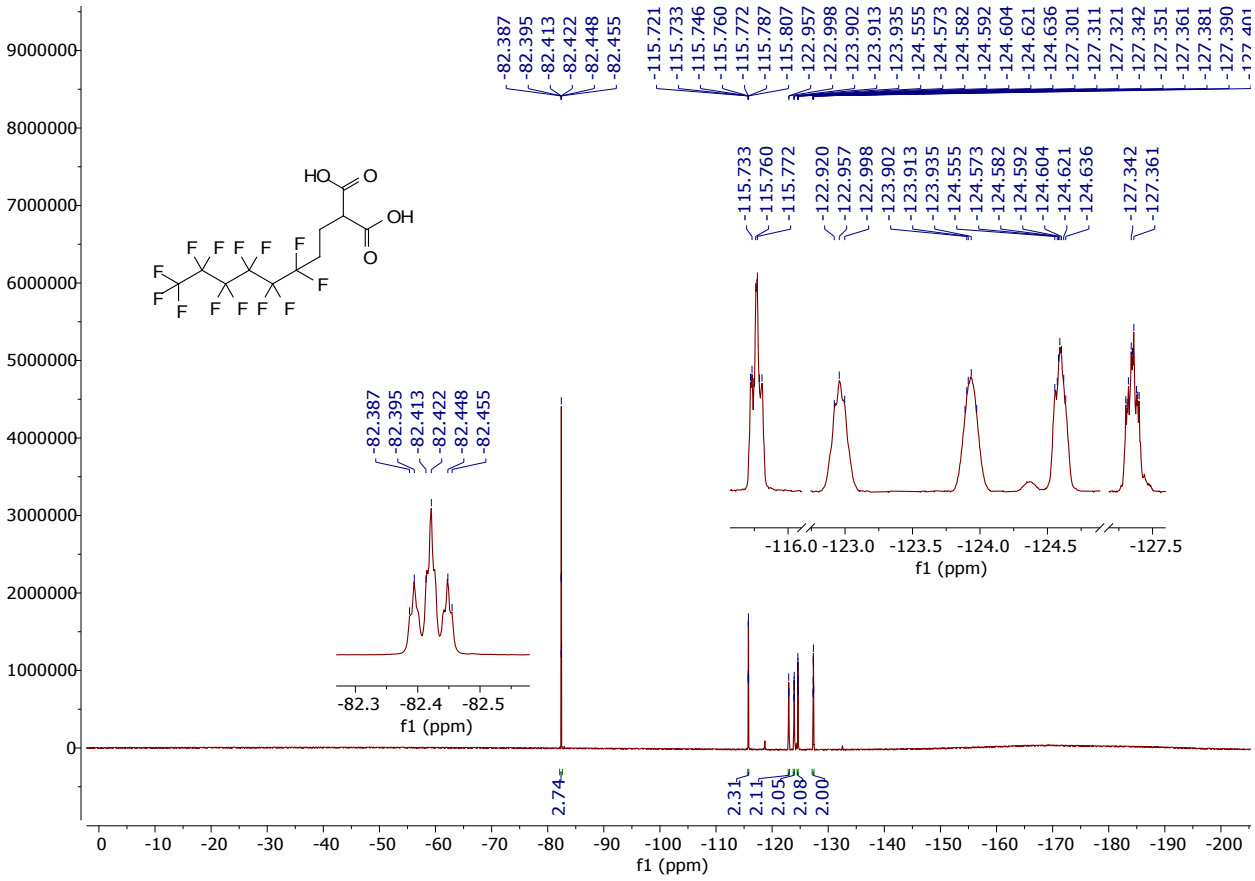

Figure S58. ^{19}F NMR spectrum of PD-12.

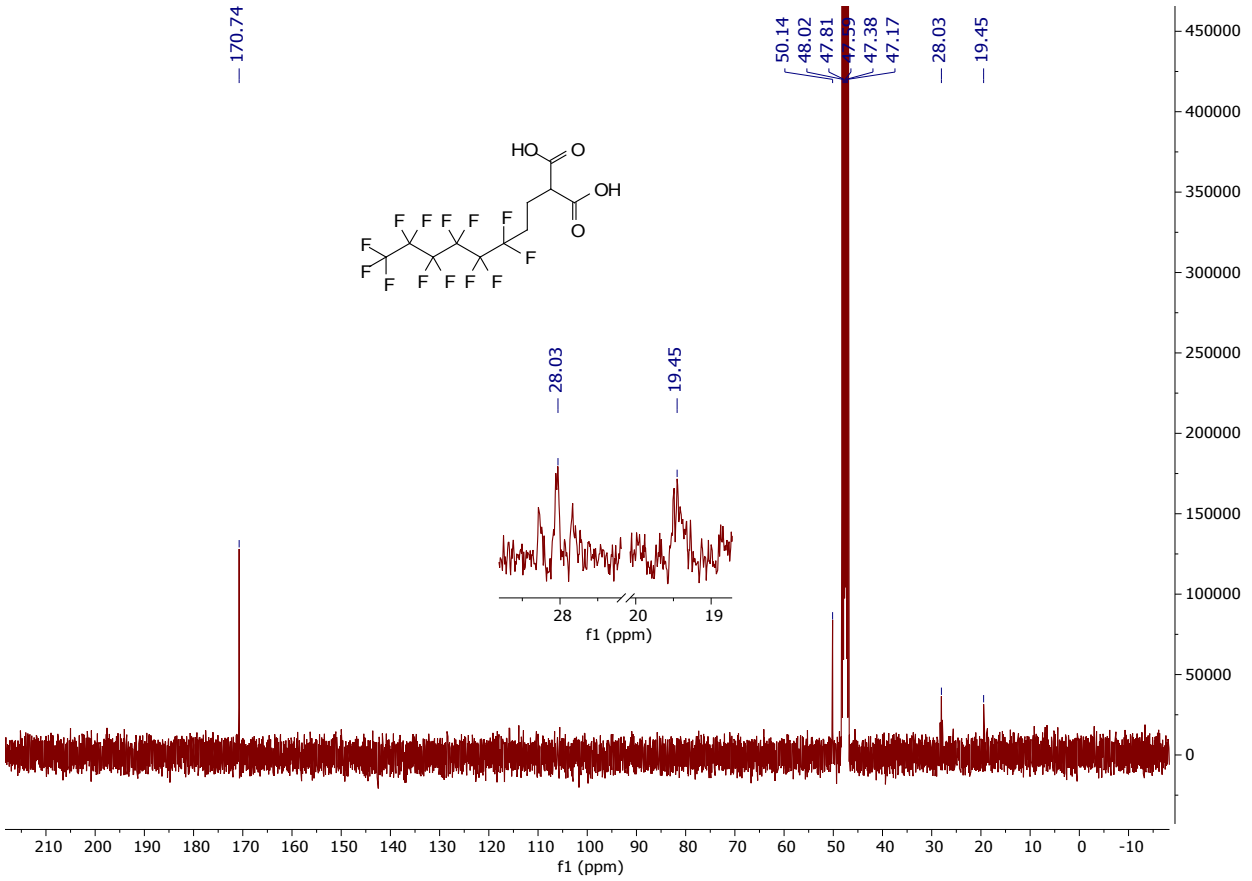

Figure S59. ^{13}C NMR spectrum of PD-12.

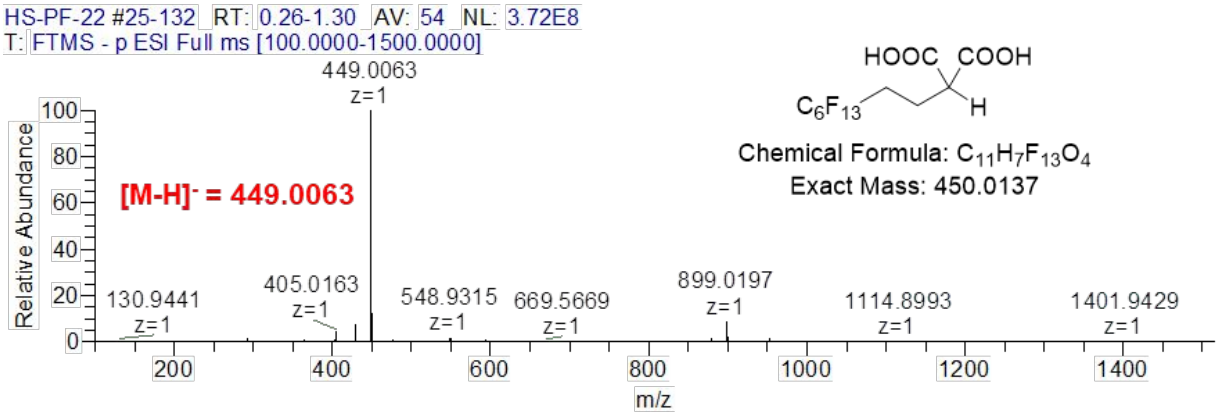

Figure S60. High resolution mass spectrum of PD-12.

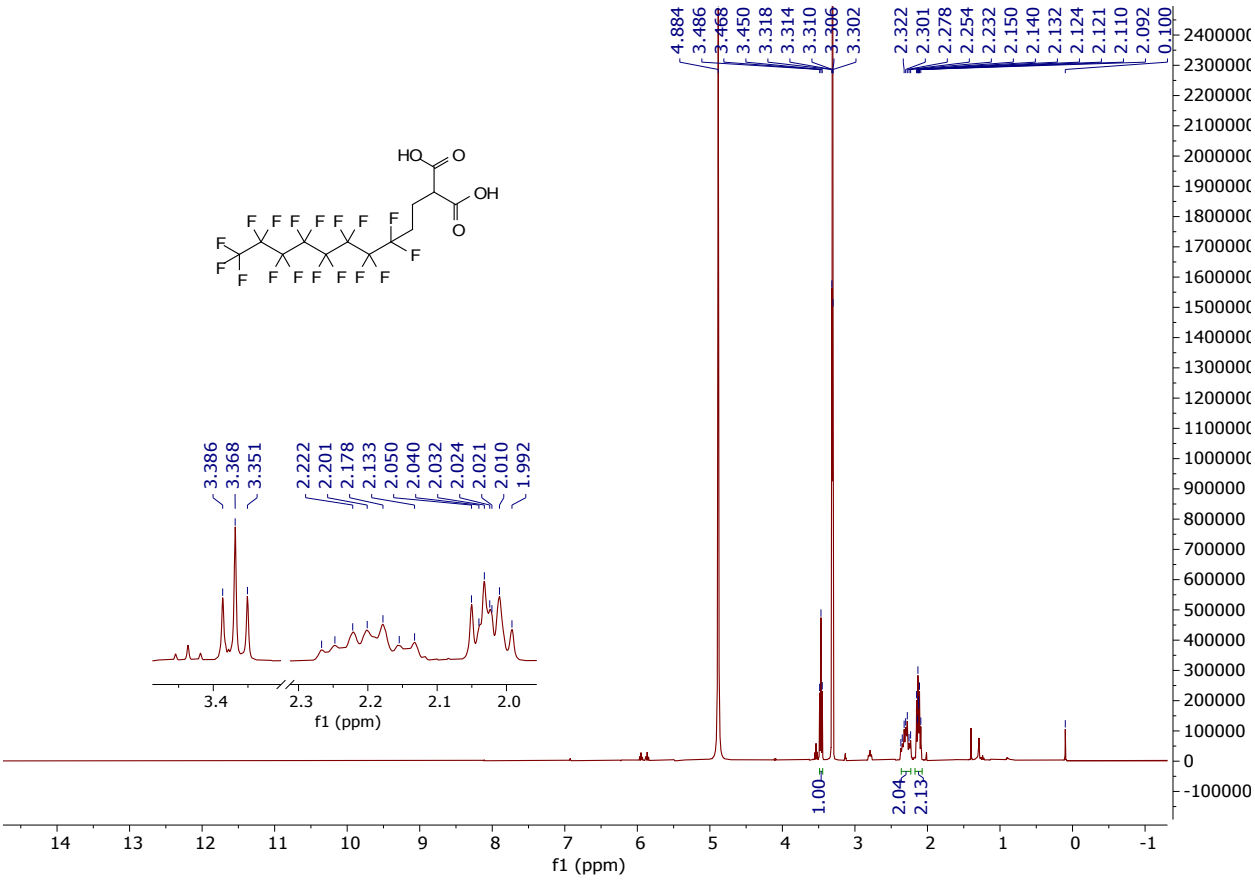

Figure S61. ^{1}H NMR spectrum of PD-13.

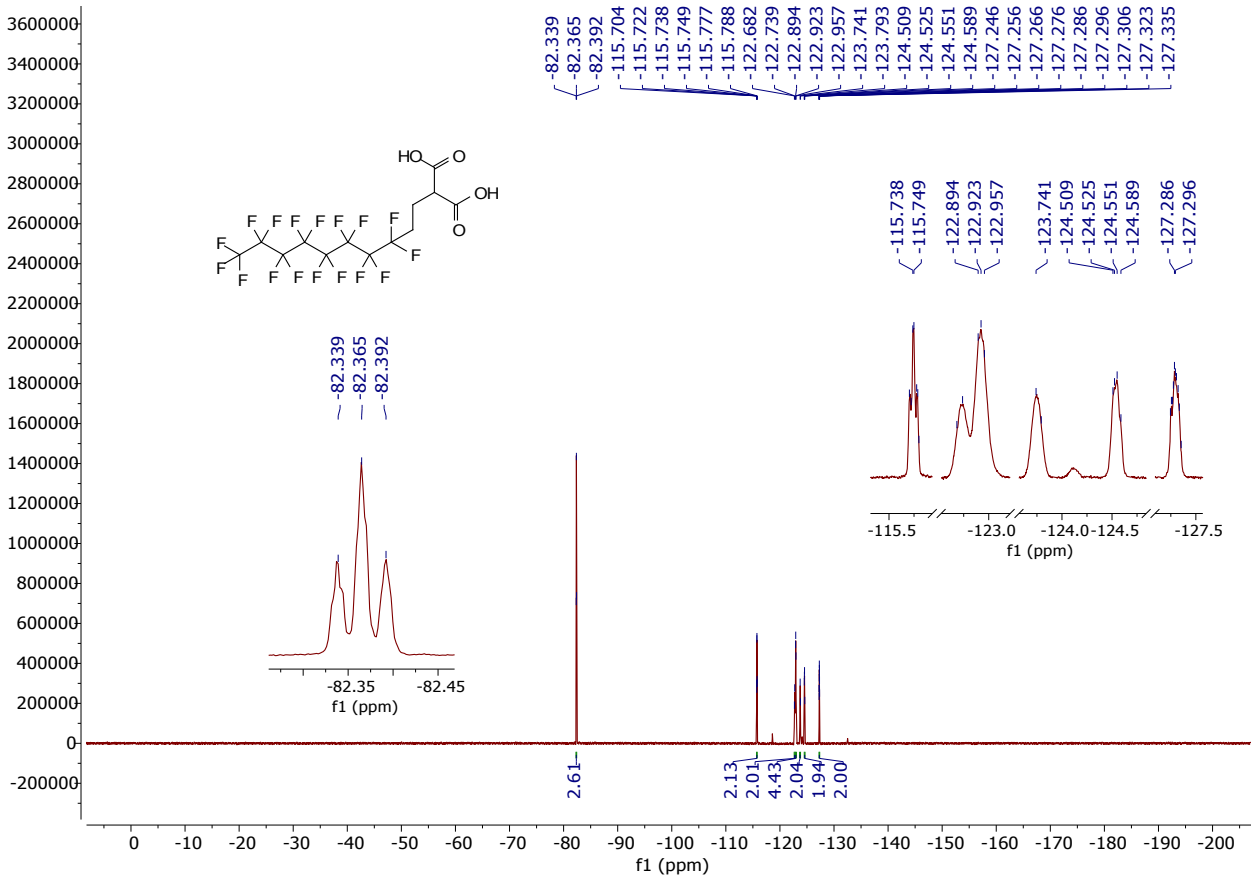

Figure S62. ^{19}F NMR spectrum of PD-13.

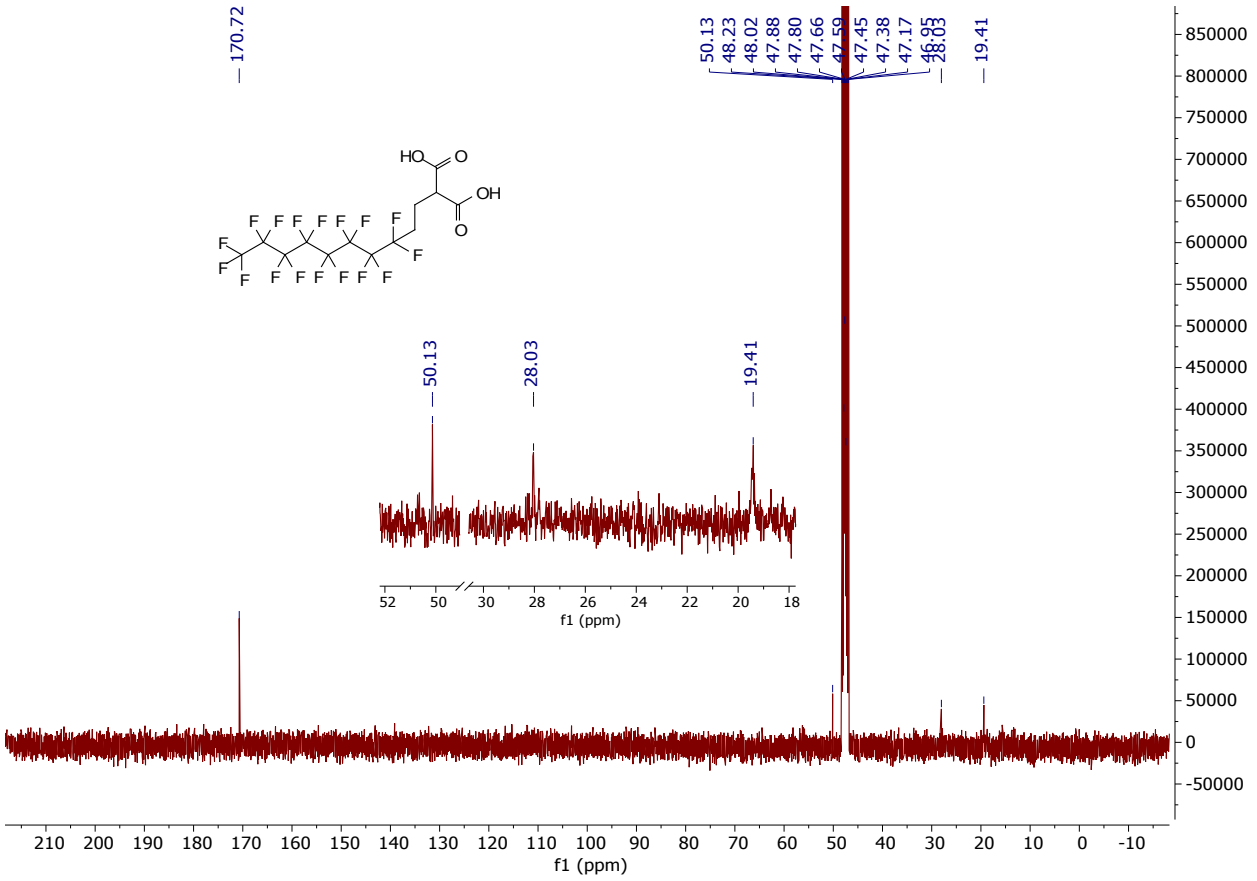

Figure S63. ^{13}C NMR spectrum of PD-13.

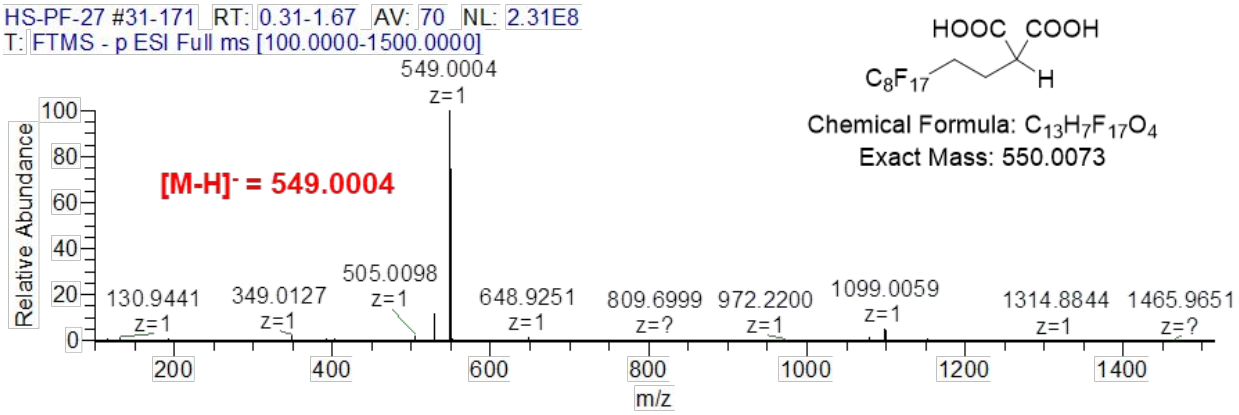

Figure S64. High resolution mass spectrum of PD-13.

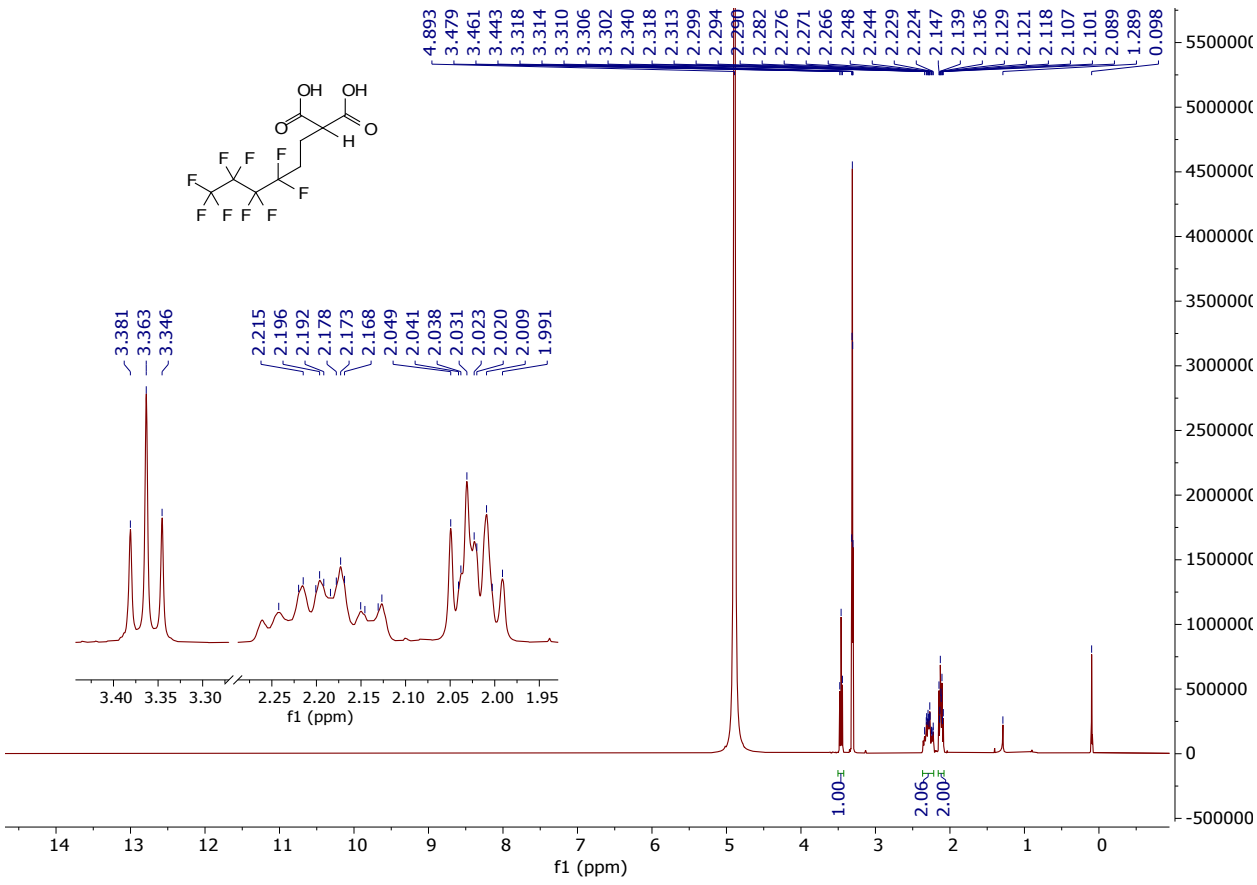

Figure S64. ^{1}H NMR spectrum of PD-14.

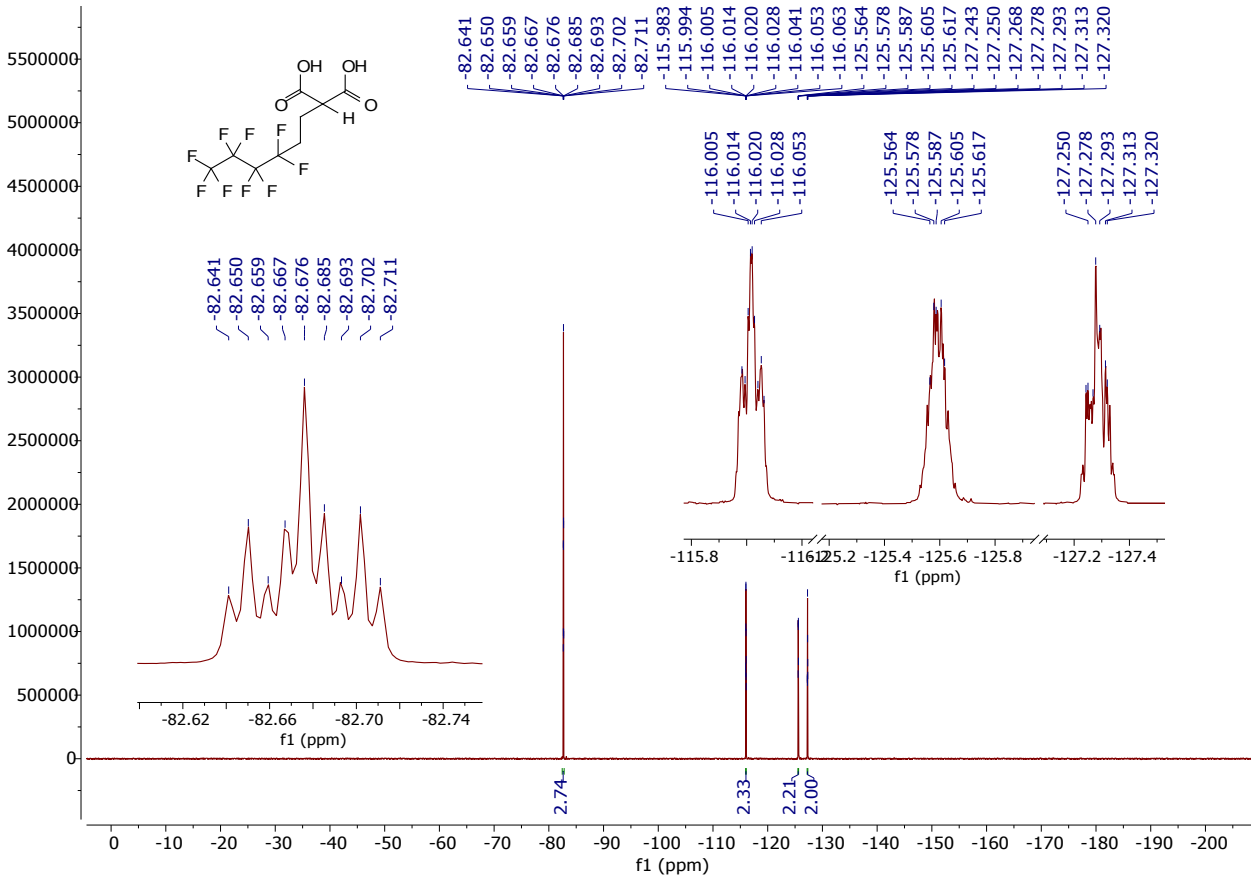

Figure S65. ^{19}F NMR spectrum of PD-14.

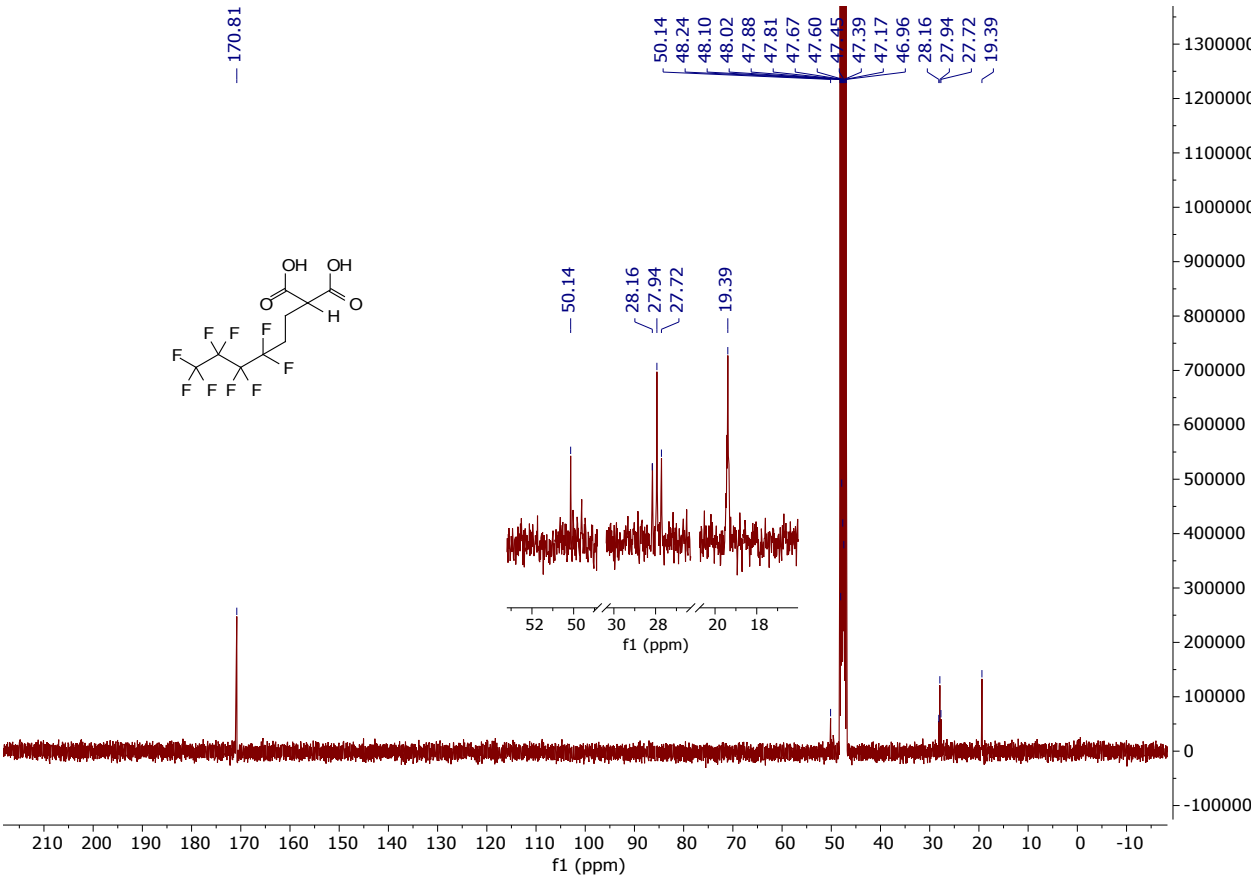

Figure S66. ^{13}C NMR spectrum of PD-14.

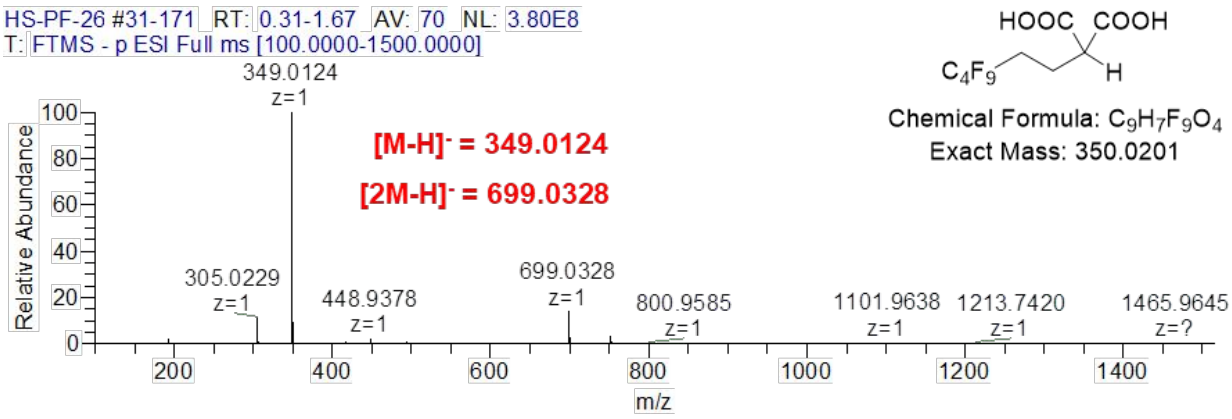

Figure S67. High resolution mass spectrum of PD-14.